



# Solar assisted gas boiler for hot water distribution system

By Antoine VOGT

Supervised by  
Dr Michael J. TIERNEY

A dissertation submitted to the University of Bristol in accordance with the requirements of the degree of Master of Science by advanced study in Mechanical Engineering in the Faculty of Engineering.

Department of Mechanical Engineering

Submitted the 16/09/2016

15857 words



## Summary

The aim of this project was to design and check the financial viability of solar pre-heating for the gas heating system of a block of Baddock Hall, a *University of Bristol* owned student accomodation. These investigations are motivated by both the rapid escalation of the rate of the *Climate Change Levy* (CCL), a tax on the consumption of fossil fuels applicable to the industry and public sector, and the probability of an increase in the price of natural gas over the next 25 years.

The solar system was designed using recommendations of CIBSE and manufacturers of solar collectors. Some 16 configurations were defined to study the influence of parameters such as the area of collector, volume of the storage tank and capacity of heat exchangers. Results of simulations prove the technical interest of solar pre-heating with monthly solar fractions of 15-35% over the period April-September and 5-15% during the rest of the year. Annually, solar fractions of 13-18% can be expected. Components such as heat exchangers and collectors appear to have the largest influence on the efficiency of the system. The analysis shows that a careful selection of components allows a reduction of the capital cost while maintaining the same efficiency.

The solar pre-heating is however not likely to offer any savings even for a scenario where the price of gas increases significantly and the University manages to get a discount on the CCL. Here, the savings are purely artificials since only due to governmental incentives. On the other hand, a decrease in the price of solar collectors might significatnly improve the profitability of solar systems. The investment on solar pre-heating for the gas unit of Baddock is then risky and not recommended.

## Author's declaration

I declare that the work in this dissertation was carried out in accordance with the requirements of the University's Regulations and Code of Practice for Taught Postgraduate Programmes and that it has not been submitted for any other academic award. Except where indicated by specific reference in the text, this work is my own work. Work done in collaboration with, or with the assistance of others, is indicated as such. I have identified all material in this dissertation which is not my own work through appropriate referencing and acknowledgement. Where I have quoted from the work of others, I have included the source in the references/bibliography. Any views expressed in the dissertation are those of the author.

SIGNED: Antoine Vogt

DATE: 16/09/2016

A handwritten signature in black ink, appearing to be 'AV', with a long horizontal stroke extending to the right.

## **Acknowledgements**

I thank Dr Michael J. Tierney for having supervised me, his professionalism and enthusiasm were of a great help during the whole process of the project.

I also acknowledge and thank Mr John Brenton for having provided useful data on the gas unit of Baddock Hall.

# Table of content

1	Introduction	12
1.1	Context of the project.....	12
1.2	Objectives .....	12
2	Literature review	14
2.1	Interest and design of solar pre-heating systems .....	14
2.1.1	Interest of solar pre-heating systems .....	14
2.1.2	Importance of stratification in tanks .....	14
2.1.3	Sizing of the plant.....	15
2.2	Demand profile and estimation of the flow-rate.....	16
2.2.1	Shape of demand profiles .....	16
2.2.2	Determination of the maximal demand.....	17
2.3	Health and safety requirements .....	17
2.3.1	HSE rules for control of water quality .....	17
2.3.2	Disinfection methods for drinking water.....	17
3	Modelling	19
3.1	Description of the plant .....	19
3.2	Stratified tank.....	20
3.3	Heat exchanger .....	22
3.4	Solar panel – Control of the solar loop.....	23
3.5	Gas boiler – Control of the heating loop .....	24
3.6	Pipework.....	26
3.7	Inputs and parameters of simulation.....	27
3.8	Validation test of the system .....	32
3.9	Financial model.....	33
3.10	Plan of numerical experiments .....	34
4	Results and discussions	36
4.1	Solar fraction and impact of components.....	36
4.1.1	Analysis of the solar fraction (monthly and annual).....	36
4.1.2	Effect of heat exchangers.....	38
4.1.3	Effect of the solar heat storage tank.....	40
4.1.4	Effect of solar collectors .....	42
4.2	Compliance with health and safety requirements .....	43
4.2.1	Load tank .....	43
4.2.2	Solar heat storage tank .....	45
4.3	Financial assessment .....	49
4.4	Recommendations for further work.....	52
5	Conclusion	55
6	References	56

Appendix A	Simulink model of the proposed solar assisted plant.....	59
Appendix B	Implementation of stratified tanks .....	60
Appendix C	Implementation of heat exchangers.....	64
Appendix D	Implementation of solar panels .....	64
Appendix E	Gas boiler and controller of the gas heating loop.....	66
Appendix F	Cost of components of the system <sup>[41]</sup> .....	67
Appendix G	Capital cost of solar pre-heating systems .....	67

## List of figures

Fig. 1	Efficiency of the two flat plate collectors selected for the study under the same operating conditions .....	16
Fig. 2	Description of the current gas heating installation of Baddock Hall block, only one the two units represented. B: gas boiler, LT: load tank, P: pump. The secondary flow [dotted] is not implemented. ....	19
Fig. 3	Description of the solar assisted gas system studied with SC: solar panel, ST: solar heat storage tank, LT: load tank, HX: heat exchanger, B: gas boiler, P: pump, $T_i$ : temperature. The secondary flow [dotted] is not implemented. ....	20
Fig. 4	Schematic representation of the heat balance (1) applied to a layer. Red and blue arrows show respectively the sense of convection flow during heating and discharging (cooling). The two grey parts represents the wall of the tank.....	21
Fig. 5	Comparison of simulated results obtained with the heat balance (1) with Alizadeh's model 15 layers [11]. Only the temperature of the top layer is plotted. Test realised with flow-rate of $11\text{l}\cdot\text{min}^{-1}$ and a tank of 300l. ....	21
Fig. 6	Diagram of control of the heating process as a function of the temperature at the bottom of the load tank $T_7$ , the temperature at the top of the solar tank $T_5$ and the output of the heating system during the previous step of simulation $Q_{\text{previous}}$ . Operation repeated at each step of simulation. ....	26
Fig. 7	Temperature evolution at the outlet of the pipe obtained during test cases on a 36m long pipe and a flow of velocity $0.58\text{m}\cdot\text{s}^{-1}$ . The QUICK scheme improves the result in time for high number of nodes but introduces overshoot.....	27
Fig. 8	Profile of hot water demand seen by one unit of the installation of Baddock Hall, defined by Knight, N. ....	28
Fig. 9	Comparison of (a) solar irradiation and (b) ambient temperature between the smoothed values of the SOLAREC-PVGIS and the real measurements made in Filton the 16 <sup>th</sup> (low irradiation) and 18 <sup>th</sup> (high irradiation) of July 2016.....	29
Fig. 10	(a) Convergence in day to day change of the temperature difference between the top and the bottom of the tank and (b) convergence in error of the energy content of tank .....	31
Fig. 11	Convergence in error between successive values of the time step for both energy content and temperature difference. ....	31
Fig. 12	Cumulative energy consumption and instantaneous power provided by the two boilers as a function of time, curves obtained with the <i>Simulink</i> model of the current gas heating Installation of Baddock Hall .....	32
Fig. 13	2015 gas price (£) projections of DECC, increased by 40% for taxes and profits, "central" and "high" scenario. ....	34
Fig. 14	Monthly solar fraction obtained for the 16 configurations of the solar pre-heating system over the six months simulated.....	37
Fig. 15	Annual solar fraction estimated by regression for the 16 configurations of the solar pre-heating system.....	38
Fig. 16	Average increase in the work of the feeding pump P1 of solar collectors when the capacity of heat exchangers (HX1) is raised from $733\text{W/K}$ to $1466\text{W/K}$ , calculated for the Riello and Solex collectors.....	39

Fig. 17	Average reduction of the work provided by the three pumps feeding the heat exchanger (P3) between the heat storage and the load tank (P4 x2) when the capacity of heat exchangers (HX1 and HX2) is raised from 733W/K to 1466W/K, calculated for Riello and Solex collectors.....	39
Fig. 18	Impact on the capital cost of the solar system of increasing the characteristics of heat exchangers compared to increasing the surface of collector by 25% in the case of Solex BLUX collectors and Riello CSAO 25R .....	40
Fig. 19	Average efficiency of the collectors over the month of May for various configurations.....	40
Fig. 20	Influence of the volume of the storage tank on annual solar fraction and capital cost of the system.....	41
Fig. 21	Increase in work of pump P1 when Riello panels are used instead of Solex ones. Storage tank of 500l and heat exchangers of 1466W/K capacity. ....	43
Fig. 22	Example of capital cost increase due to the selection of high efficiency solar collectors (Riello) and its impact on annual solar fraction.....	43
Fig. 23	Example of rate of energy transfer from the heat storage tank to the load tank during the month of May, 20m <sup>2</sup> of Riello collectors, storage volume of 500l and heat exchangers at 1466W/K.....	44
Fig. 24	Temperature development of the top and bottom layers of the load tank during heating process in two cases: low and high heat content in the heat storage tank. 20m <sup>2</sup> of Riello collectors, storage volume of 500l and heat exchangers at 1466W/K. Layer 1 standing for the top of the tank and layer 20 for its bottom.....	44
Fig. 25	Temperature of the layers of the one load tank during a day of May, layer 1 being the top of the tank and layer 20 its bottom. 20m <sup>2</sup> of Riello collectors, storage volume of 500l and heat exchangers at 1466W/K.....	45
Fig. 26	Simulated temperature profile in the heat storage tank during the month of November when 20m <sup>2</sup> of Solex collectors, large heat exchangers (1466W/K) and a storage volume of (a) 400l, (b) 500l .....	46
Fig. 27	Simulated temperature profile in the heat storage tank during the month of March when 20m <sup>2</sup> of Solex collectors, large heat exchangers (1466W/K) and a storage volume of (a) 400l, (b) 500l .....	47
Fig. 28	Simulated temperature profile in the heat storage tank during the month of May when 20m <sup>2</sup> of Solex collectors, large heat exchangers (1466W/K) and a storage volume of (a) 400l, (b) 500l .....	48
Fig. 29	Expected savings of various configurations of solar pre-heating relatively to the current installation of Baddock Hall. Different types of funding are considered (a) amortisation over 25 years at a rate of 6%, (b) amortisation over 7 years at a rate of 3.3% and (c) payment of the capital at the installation (no loan).....	50
Fig. 30	Savings in various scenarios of gas cost and funding if the price of Riello CSAO 25R collectors was the same than Solex BLUX collectors. Configuration with 16m <sup>2</sup> of collector, storage tank of 400l and heat exchanger of transfer coefficient UA = 1433W/K. ....	52

## List of tables

Table 1	Characteristics of the two heat exchangers used in the simulations, <i>Northern Lights</i> [38] .....	23
Table 2	Configurations of the solar pre-heating system used for simulations....	34
Table 3	Extremum of heat content for various volumes of solar heat storage tanks.....	41
Table 4	Simulated efficiency of solar collectors over the month of May 2016, depending on the volume of the storage tank (ST) and the fraction of volume allocated per m <sup>2</sup> of collector.....	42
Table 5	Payback time and expected savings of the three solutions reaching economic viability in the case of a funding with an amortisement over 7 years at 3.3% and scenario 4. ....	49
Table 6	Payback time and expected savings of the six best solution in the case of scenario 3 with payment of the capital at the installation of the system. ....	51

## Nomenclature

$A_c$	Solar collector area [m <sup>2</sup> ]
$A_{ex}$	Exchange surface of the heat exchanger [m <sup>2</sup> ]
$A_{tank}$	Surface of the longitudinal section of the tank [m <sup>2</sup> ]
$c$	Specific heat of water [kJ.kg <sup>-1</sup> .K <sup>-1</sup> ]
$G$	Solar irradiation [W.m <sup>-2</sup> ]
$\dot{m}$	Flow-rate through the tank [kg.s <sup>-1</sup> ]
$\dot{m}_c$	Mass flow-rate of heat exchange fluid through collectors [kg.s <sup>-1</sup> ]
$P$	Perimeter of the tank [m]
$Q_{boiler}$	Heat transfer rate of the boiler [W]
$Q_{max}$	Maximal heat transfer between the two fluids [J]
$t$	Time [s]
$T$	Temperature of the layer [°C]
$T_a$	Temperature of outdoor ambient air [°C]
$T_{amb}$	Temperature of indoor ambient air [°C]
$T_{cold, in}$	Inlet temperature of the cold fluid [°C]
$T_{hot, in}$	Inlet temperature of the hot fluid [°C]
$T_{in}$	Temperature of water at the inlet of the boiler [°C]
$T_{out}$	Temperature of water at the outlet of the boiler [°C]
$T_m$	Temperature of the solar collector [°C]
$\Delta T$	Temperature difference between inlet and outlet of solar collectors [°C]
$U_{ex}$	Overall heat transfer coefficient of the heat exchanger [W.K <sup>-1</sup> .m <sup>-2</sup> ]
$U_{tank}$	U-value of the insulation of the tank [W.K <sup>-1</sup> .m <sup>-2</sup> ]
$\Delta x$	Thickness of layers [m]
<i>Greek symbols</i>	
$\eta$	Efficiency of the solar collector [%]
$\lambda$	Thermal conductivity of water [W.m <sup>-1</sup> .K <sup>-1</sup> ]
$\rho$	Density of water [kg.m <sup>-3</sup> ]

# 1 Introduction

## 1.1 CONTEXT OF THE PROJECT

In the UK, 18% of the energy consumed in the residential sector is used for heating “consumption” water [1], i.e. water used by showers, sinks, basin, washing machines, ... For institutions like the *University of Bristol*, owner of several halls of residence housing thousands of students, the energy bill for hot water is substantial. At the same time, 99% of the domestic energy is produced with fossil fuels (68% for gas, 22% for electricity, 7% for oil, 1.5% for coal and other solid fuels) [2] for which resources and for which their combustion results in global warming.

Since 2001, both industry and the public sector paid an environmental tax on every kilowatt-hour (kWh) of fossil fuel energy consumed. Named the *Climate Change Levy* (CCL), this tax aims to encourage the shift toward more responsible and eco-friendlier ways of producing and using energy. The rate of the CCL, fixed by the UK government, is capped to avoid affecting the competitiveness of business and institutions targeted by this tax, yet an important increase of the rate will occur between 2016 and 2019 (+73% for natural gas and oil, +51% for electricity) [3]. The growing concerns about climate change lets us predict that the rate will continue increasing at least over the next decade. Additionally, the cost of fossil fuels can vary steeply and unpredictably, the worldwide increase in energy is in any case likely to raise the cost of all fuels.

Solutions exist to reduce the escalation of the energy bill. Firstly, the UK government proposes a deal named *Climate Change Agreement* (CCA) in which the company or institution commits to engage policies in favour of a progressive reduction in energy consumption. With a CCA, discount on the CCL of 78% for gas and oil and 93% on electricity can be granted.

The second solution is to adapt the heating system for a renewable source of energy. In England, the *Renewable Heat Incentive* (RHI) is a payback scheme designed to entice the installation of renewable systems, often blocked by the high cost of necessary investment. For every new renewable heating system installed by a licensed professional, the state will pay the householder during the 7 first years for every kWh of renewable energy produced [4].

Baddock Hall of residence is owned by the *University of Bristol*. It comprised from different blocks, in which live in average 40-50 students. Each block is equipped with its own water heating system. The building having been built in the 1960's, at a time where energy savings were not a priority, most of its heating systems are not modern. Thus, the *Sustainability Service* of the University has been working actively on finding new solutions to replace the old and obsolete electric heaters. Most of them have now been replaced by heat pumps or condensing gas boilers. Baddock Hall has then become a pilot project for the introduction of renewables.

A study was recently made to determine the most profitable solution for a refit of the electric installation. The conclusion was drawn that significant savings were able to be made by changing for solar heating or heat pumps. However, the study did not investigate whether the combination of renewables and gas boiler was profitable. The survey also produces more rigorous dynamic models of the thermal systems (implemented in the Simulink environment) than the previous work done at Baddock Hall.

## 1.2 OBJECTIVES

The present project had three main objectives: to develop a reliable simulator for a solar assisted gas boiler, to evaluate the achievable solar fraction and to assess

financially the viability of the system. The project should help the *Sustainability Service* of the university in their further plans of refitting installations.

This project could have been done by using *TRNSYS*, a simulation software for heating systems. But, to be able to know and understand the underlying theory of the components of the system, the choice was made to build from first principles a model on *Simulink*. As opposed to *TRNSYS*, *Simulink* is accessible on every computer of the University, the model can then be more easily and conveniently re-used. Obviously, the model developed here is intended to be the base of further studies at Baddock Hall or on other sites.

Secondly, the project aims to determine the solar fraction achievable by a solar pre-heating system, designed according to the guidelines of manufacturers and official institutions, and to investigate the influence of the different components on its efficiency.

The final objective is to quantify the potential savings the solar system can provide (if any) compared to the current gas heating installation. From the results, it will be concluded if the investment is risky or not and whether there is any financial interest in switching to that type of system.

The spectrum of analysis is wide. Also if the present study is mostly oriented toward Baddock Hall's plant and associated problematics, it aims to be useful in the more general context of high occupancy buildings.

## 2 Literature review

The literature review was submitted for examination in December 2015. The general topics covered where: the patterns of water consumption, the theory of storage tanks, the means for water disinfection... Here are summarised the key features that are essentials to the understanding of the current project.

### 2.1 INTEREST AND DESIGN OF SOLAR PRE-HEATING SYSTEMS

#### 2.1.1 *Interest of solar pre-heating systems*

The principal problem of solar systems is their high capital cost, making difficult to do savings when energy production is not high all over the year. When it comes to large buildings, full solar heating with electric or gas backup heater, which requires large surface of collector (1-1.5m<sup>2</sup> per person [5]), are not well fitted for northern Europe where a large variation in solar insolation level happens between summer and winter.

Solar pre-heating does not aim to provide most of the energy required but less than a half in general. The objective is to pre-heat water, as much as possible, to reduce the energy consumption of the boiler making the balance. The surface of collector required drops to 0.32-0.4m<sup>2</sup> [6] per person and so the capital cost. Pre-heating is recommended for northern Europe as it is more likely to provide savings than full heating.

#### 2.1.2 *Importance of stratification in tanks*

##### ➤ *Basic knowledge on stratification*

The stratification of water is a natural gravity-led process. When water is heated buoyancy will lead hot water at the top of the tank and cold water at its bottom. A thermocline, layer of water in which a steep gradient of temperature occurs, separates the hot and cold volumes [7].

The formation of stratification is complex, delicate and still misunderstood. Operating conditions of the tank (inlet and outlet flow), design of the tank (geometry, dimensions) and additional devices (such as diffuser plates) are found to have a great influence on the ability of stratification to appear and its quality. An extensive review of the current knowledge on stratification can be found on ref. [8].

In solar systems, stratification in tanks is wanted as it increases the exergy (quality of heat) of water and it allows solar collectors to work at cooler temperature, where they are more efficient.

##### ➤ *Modelling of stratification*

Various mathematical models of stratification can be found in published literature. The choice depends on the effects to study (temperature, flows...) and on the computational power available.

One-dimensional models are common and known to give a sufficient precision. They consist in studying the gradient of temperature along the height of the tank. They consist in dividing the volume inside of the tank in a definite number of layers on which are applied heat balances. The heat balance embeds conductive and convective effects with the tank and other layers, the expression of the heat balance can vary depending on the completeness of the modelling. If the heat balance is generally used under the form of a differential equation [9-10] some work has been done to determine iterative expressions easier to use [11]. However, one-dimensional models are purely based on thermodynamics considerations and will not take into account the effects of mixing due to inlet and outlet flows for example.

A static behaviour of a tank will then be properly modelled, while it is less certain for a dynamic one. Yet one-dimensional models are reportedly implemented in TRNSYS, the famous software of heating system simulation.

Contrary to one-dimensional models, two and three-dimensional ones are able to give the evolution of the temperature in every point of a section of the tank. Then the effects of mixing and flows can be modelled. This improvement allows the study of tanks with complex geometries and the effect of diverse obstacles in the tank. In practice, the use of a such models shall be justified by specific needs because of the significant increase in the computing cost implied.

### **2.1.3 Sizing of the plant**

#### **➤ Load tank, storage of hot water to be distributed**

For gas heating systems, the *Chartered Institution of Building Services Engineers* (CIBSE) recommends to size the storage of hot water proportionally to the expected peak demand of the day and to ensure a recovery time of 30min (time to get back to a fully heated situation) [12]. According to the audit made on site by the company Ferguson-Brown, the current installation of Baddock Hall (two gas boilers of 61kW and two tanks of 325l), which is slightly oversized, meets these requirements [13].

#### **➤ Solar heat storage tank**

When solar-preheating is associated to a gas system, CIBSE and manufacturers [12] recommends the use of a separate tank to store the energy harvested by solar panels. This aims to increase the time of use of the solar system and then its profitability. The volume of the storage tank has to be proportional to the area of panel installed. *Buderus*, a German manufacturer of solar systems (subsidiary of Bosch), recommends to allocate a minimum of 20l per m<sup>2</sup> of collector [14], while SPF values are in the range 20 l.m<sup>-2</sup> to 25l.m<sup>-2</sup> [6]. These volumes are determined in order to optimise the time of heating, the quantity of energy harvested, and the quality of heat (exergy).

#### **➤ Solar collectors**

Two different types of solar collectors dominate the market: flat plates (FPC) and evacuated tubes (ETC). In spite of being in general two times more expensive than FPC, ETC does not improve significantly the quantity of energy harvested by the system each year [15]. Only FPC will then be considered in this project.

The *Institut für Solartechnik* (SPF) prescribes a surface of flat plate collectors between 64 m<sup>2</sup> and 80 m<sup>2</sup> for 200 people to reach an expected solar fraction of 25% at peak [6]. Assuming a linear relationship between surface of collectors and the number of people, the studied unit of Baddock Hall would require between 16 m<sup>2</sup> and 20 m<sup>2</sup> of flat plates.

The characteristics and prices of FPC vary grandly depending on the brand and the design. Investigations in the open database of SPF show two big categories of FPC: the standard and the very efficient ones. For the purpose of the project one reference of both of these categories is selected:

- High efficiency collector: Riello CSAO 225R
- Standard-low efficiency collector: Solex BLUx

The SPF test report for the two previous reference are respectively accessible in ref. [16] and [17].

The price per m<sup>2</sup> of Riello collector is estimated 200£ more expensive than the Solex [18-19]. Fig. 1 shows the efficiency of the collectors under the same operating conditions.

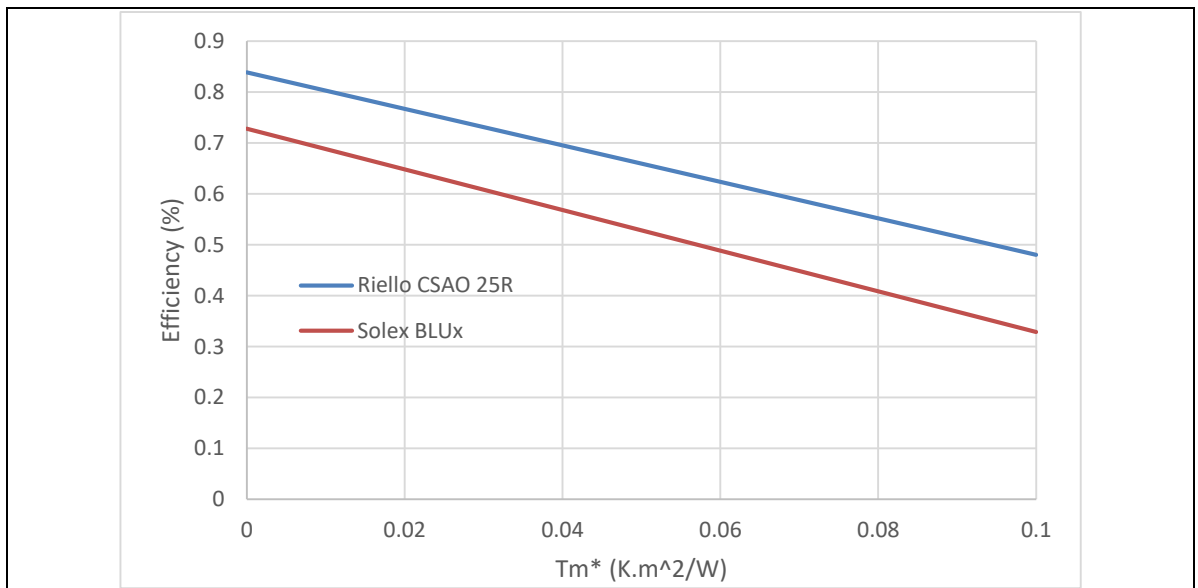


Fig. 1 Efficiency of the two flat plate collectors selected for the study under the same operating conditions

### ➤ **Heat exchangers**

Three main type of heat exchangers are commonly used for water heating: immersed coils, mantles and external heat exchangers [8].

In solar systems, the immersed coil heat exchanger of the solar loop (circuit of collectors) is generally placed at the bottom of the tank, this allows to heat the naturally coldest part of the tank. Only low gradients of temperature between the top and the bottom of the tank can be achieved (around 15°C maximum), synonym of weak stratification. Mantle heat exchangers, transferring heat through the wall of the tank, have shown encouraging results compared to immersed coils from the point of view of efficiency and gradient of temperature. However, the stratification is perturbed by the transfer of energy to the cold layer.

The most appropriate solution is to use external heat exchangers. They allow high transfer rates of energy and do not perturb the stratification as much as the previous solutions. The main interest is the possibility to locate precisely the inlet and outlet of water in the storage tank, and therefore to grandly improves the gradient of temperature. For solar applications, the use of counter-flow plates heat exchangers seems to be common (compact, high effectiveness). The drawback of external heat exchangers compared to the previous solutions is the need for an additional pump in the system and extra length of pipes. This technical solution being the most widely used, it was chosen for this study.

## **2.2 DEMAND PROFILE AND ESTIMATION OF THE FLOW-RATE**

### **2.2.1 Shape of demand profiles**

In the UK, the average daily hot water consumption per person in households was of 122l in 2015 [20]. In Baddock Hall however, metrics show that the consumption peaks at 40l/day/capita [13]. The difference can be explained by the fact that washrooms are common to several dormitories and then likely to be used in less convenient conditions than “at home”.

Daily patterns of consumption are comprised from peaks distributed all over the day. These peaks generally happen at periods of high occupancy of the building [21-22].

Four peaks are identified at Baddock Hall: between 08:30 and 10:00, 12:00 and 13:00, 15:00 and 16:00 then at 18:00 to 19:00, the consumption between them is negligible. It is easily noticed that these peaks correspond to hours at which student are not likely to have class. Reportedly, the maximum draw-off over half an hour at peak reaches 250l for 45-50 students.

### **2.2.2 Determination of the maximal demand**

A correct estimation of the maximal demand flow-rate allows to design properly the distribution system (tanks, pipes ...) and ensure satisfactory functioning for users.

The “fixture unit” approach is a convenient method to calculate the maximal flow-rate an installation should be able to provide with a risk of error of 1% [23]. Each appliance (sink, basin, shower rose) is associated to a value depending on its characteristics (diameter of pipes, time of use...), the sum of all the values allows the determination of the probable maximal flow-rate thanks to abacus defined with probability theories. In the UK, data for calculations are provided by the *Chartered Institute for Plumbing and Heating Engineering* (CIPHE).

However, the “fixture unit” approach overestimates by 50 to 60% the maximum flow-rate when more than 20 washrooms are involved. In these cases, the use of Monte-Carlo simulations is more appropriate and gives outstanding results for predictions [24]. This method yet requires more resources for both the creation of a database and the computation.

## **2.3 HEALTH AND SAFETY REQUIREMENTS**

Hot water is naturally a favourable environment for the growth of viruses, bacteria and micro-organisms which can be hazardous for humans. Basic rules and disinfection method have been developed to control and guarantee the quality of water distributed by the heating system.

### **2.3.1 HSE rules for control of water quality**

The *Health and Safety Executive* (HSE), a UK governmental agency, has published guidelines relative to storage of water and *Legionella* bacteria control. It specifies that cold water must be stored below 20°C and hot water above 60°C continuously. Additionally, water has to be distributed from the tank to the outlet of appliances in less than one minute and remain above a temperature of 50°C [25-26].

The *Water Regulations Advisory Schemes* (WRAS), an association formed by the UK water suppliers, recommends to heat up the entire volume of a storage tank at 60°C during at least one hour per day to avoid any outbreak. This rule, less strict than HSE's one, is allegedly sufficient for ensuring safety [27].

Thermostat in storage tanks and secondary flow circulation in pipework are simple solutions which allow keeping water at safe temperature in every part of the distribution system.

### **2.3.2 Disinfection methods for drinking water**

The continuous thermal treatment of water is efficient, but in some cases it cannot be sufficient or high enough temperature level cannot be reached. Physical or chemical disinfection processes can be used as backup solutions.

#### **➤ Chemical treatments**

Chemical treatments are mostly affected by the pH, the temperature, the contact time and the presence of interfering surfaces. The reactions and the dynamics associated are extensively explained in books given in ref. [28-30].

Chlorine ( $\text{Cl}_2$ ) is the most widely used chemical for disinfection. When mixed with water, chlorine decays in hypochlorous acid  $\text{HClO}$  and hypochlorite ion  $\text{OCl}^-$  both responsible for the disinfection. A concentration of  $20\text{-}50\text{mg.l}^{-1}$  is able to eradicate *Legionella* with an efficiency of 99.99% [31]. Residuals of  $0.1$  to  $1.5\text{mg.l}^{-1}$  of free chlorine in water are enough to control the growth of the bacteria after treatment. Despite being cheap and not presenting concerning issues for human health, the treatment tends to attack pipes and tanks and to give taste and colour to water.

Iodine ( $\text{I}_2$ ) can also be used as a disinfectant. The radicals released are more stable in water than “free chlorine”, hence their action will then last longer. Furthermore, iodine does not colour or give taste to water below concentration of  $16\text{mg.l}^{-1}$ . However, to reach the same level of disinfection the dose of iodine has to be twice the dose of chlorine, making this treatment more expensive than a standard chlorination.

Bromine ( $\text{Br}_2$ ) presents the same pattern of reaction and levels of efficiency than chlorine. Free bromine residuals at a concentration of  $0.1$  and  $1.5\text{mg/L}$  is able to eradicate *Legionella* in a water system [31]. Yet, the reactions with water also lead to the formation of small quantities of by-products hazardous for human health. Besides this concern, the price of the treatment is higher than chlorine, applications of bromine are then limited.

#### ➤ **Physical treatment**

The main advantage of physical treatments is the absence of unwanted reactions leading to the formation of by-products. Among the various techniques, two methods seem to have a promising future: UV and ultrasounds [32].

UV light with wavelength in the range  $240\text{-}280\text{nm}$  has interesting properties for the control and eradication of bacteria and viruses in water. By damaging their DNA, UV either kill or at least inactivates their reproductive functions. A dose of  $25\text{-}40\text{W.s.m}^{-2}$  is considered to give an acceptable bacteriological quality [29].

Ultrasonic disinfection uses the cavitation effect. In the range  $20\text{-}100\text{kHz}$ , ultrasonic generate shock waves which destruct both membrane and DNA of bacteria and viruses [33-34] Unfortunately, no information on the use of ultrasonic to treat *Legionella* contaminated water are available.

Physical treatments suffer from some drawbacks. They are energy-consuming and do not let residuals into the treated water, which can therefore be re-contaminated directly after the treatment. Thus their use is generally combined with chemical treatments, allowing then to reduce both the dose of chemical and the energy consumed.

## 3 Modelling

### 3.1 DESCRIPTION OF THE PLANT

The study focuses on the comparison between the present gas heating installation of Baddock Hall and a proposed solar assisted version. These two systems are implemented in *Matlab/Simulink*.

#### ➤ **Present installation of Baddock Hall**

According to a report written by Ferguson-Brown consultants, the current installation is less than five years old and comprises two sets of tank-plus-boiler (325 litres capacity and 61 kW power input respectively).

One of the two units is represented in Fig.2.

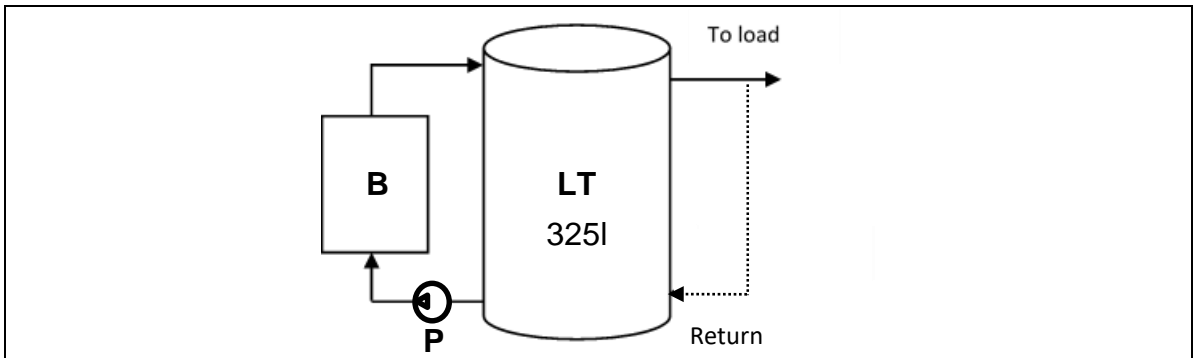


Fig. 2 Description of the current gas heating installation of Baddock Hall block, only one the two units represented. B: gas boiler, LT: load tank, P: pump. The secondary flow [dotted] is not implemented.

The purpose of a secondary flow is to maintain water in the pipework above a minimum temperature to ensure both safety (by keeping water above HSE thresholds) and rapid availability of hot water at appliances. This is performed by making hot water circulate in the pipework at a flow-rate designed to compensate the heat losses. Water drawn off the tank for this purpose ultimately comes back to it. No information about the pipework (length, diameter, insulation, material of pipes) and neither on the secondary flow loop (flow rate, working schedule) were accessible. This flow loop was therefore ignored in the model developed here.

No data relative to the insulation of tanks were available, the insulation of tanks was therefore designed using the recommendation of the US Department of Energy which specifies a minimal R-value of  $24 \text{ h}\cdot\text{ft}^2\cdot^\circ\text{F}\cdot\text{Btu}^{-1}$  ( $4.22 \text{ K}\cdot\text{m}^2\cdot\text{W}^{-1}$ ) [35]. Polyurethane foam was chosen as it appears to be widely used for tanks insulation due to its numerous advantages (inert, cheap, low conductivity). Results of Jarfelt, U. and Ramnäs O. (2006) [36] on the thermal conductivity of polyurethane foam allowed concluding that a thickness of 105 mm was sufficient to meet the insulation requirements of the US agency.

#### ➤ **Proposed solar preheating – gas system**

The plant diagram is given in Fig.3 and the implementation in Simulink in Appendix A. The base of the actual installation is kept as for solar pre-heating assisted heating systems the load storage and auxiliary heating have to be sized depending on the demand, which is independent of the source of energy [12].

The proposed plant adds new features to the current gas heating system: solar collectors (SC), two heat exchangers (HX1 and HX2) and a storage tank (ST). Solar collectors harvest solar energy and transfers the heat recovered to the storage tank by the intermediary of heat exchanger HX1. When the load tank (ST) requires heating, if enough energy is available in the tank ST, pumps p3 and p4 feed the heat

exchanger HX2 to pre-heat water. Once heat in the storage tank drops below a definite threshold, a controller activates the gas boiler to make the energy balance and raise the temperature of water in the tank LT at the reference set by the householder.

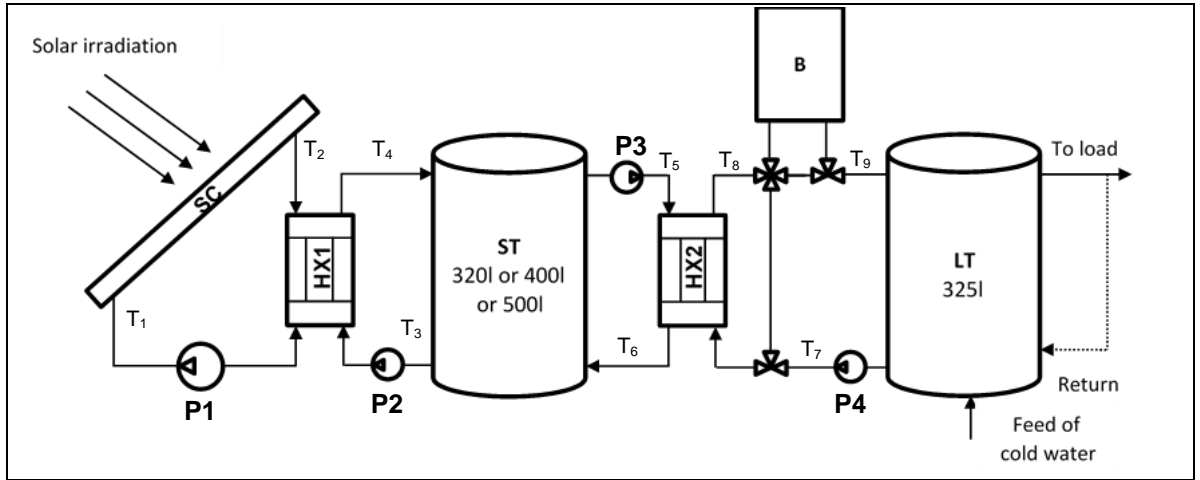


Fig. 3 Description of the solar assisted gas system studied with SC: solar panel, ST: solar heat storage tank, LT: load tank, HX: heat exchanger, B: gas boiler, P: pump,  $T_i$ : temperature. The secondary flow [dotted] is not implemented.

### 3.2 STRATIFIED TANK

All tanks are considered being stratified (a requirement for the solar heat storage and an assumption for the load storage according to Ferguson-Brown's report). One-dimensional modelling is chosen as it is known for giving valid results and was the most suitable to the computational power available during the project.

To model stratification in a tank, the volume of water it contains is divided into  $N$  horizontal layers. The evolution of temperature of each of these layers is governed by the heat balance (1) [9] which encompasses the convective and conductive heat transfers with the layers above and below, and also the heat losses through the insulation of the tank (this balance is similar to the one implemented in TRNSYS). A schematic representation is given in Fig. 4. It is implemented in *Simulink* with an S-files function (which code is provided in Appendix B for the two tanks) to estimate the time rate of change of temperature - *Simulink* then integrates this rate of change.

$$\frac{\partial T}{\partial t} = -\frac{\dot{m}}{\rho \cdot A_{tank}} \cdot \frac{\partial T}{\partial x} + \frac{\lambda}{\rho \cdot c} \cdot \frac{\partial^2 T}{\partial x^2} + \frac{U_{tank} \cdot P_{tank}}{\rho \cdot A_{tank} \cdot c} \cdot (T_{amb} - T) \quad (1)$$

Convection only applies when water is introduced or drawn off the tank (i.e. when the flow-rate  $\dot{m}$  is non zero), conduction heat losses always apply. Nonetheless, convective heat transfer, when present, is several orders of magnitude greater than conduction as predicted by Alizadeh, S. (1999) [11].

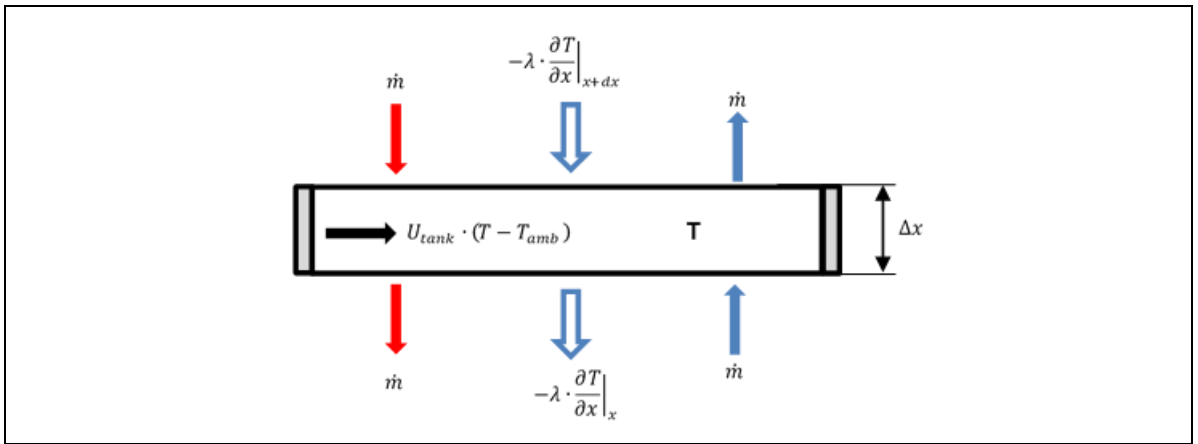


Fig. 4 Schematic representation of the heat balance (1) applied to a layer. Red and blue arrows show respectively the sense of convection flow during heating and discharging (cooling). The two grey parts represents the wall of the tank.

Each tank is equipped with an inlet selector capable of injecting inlet water at such a height as to ensure neutral buoyancy (i.e. in the layer with the adequate temperature). The use of such a device is particularly relevant when solar panels are involved, as water passing through the heat exchanger and returning to the tank is not necessarily at the same temperature or hotter than the top of the tank. Therefore, it secures the stratification and prevents the destruction of exergy by mixing water at different temperatures

The model of stratification was tested with a cycle of heating and draw-off. The first significant observation was that an increase in the number of layers, from 15 to 20, was necessary to match the results of Alizadeh, S. (1999) on temperature evolution. This is due to numerical diffusion which artificially augments diffusion coefficients. However, provided that its impact is limited, numerical diffusion can partially offset the non-consideration mixing owing to turbulent dispersion. With 20 layers, 77% of the volume of a fully heated tank at 65°C is available at the output at a temperature above 60°C. In *Guide G*, CIBSE suggest a value of 80% of the content of a stratified tank effectively available at the output at an acceptable temperature. Then the number of 20 layers was considered sufficient (see Fig. 5).

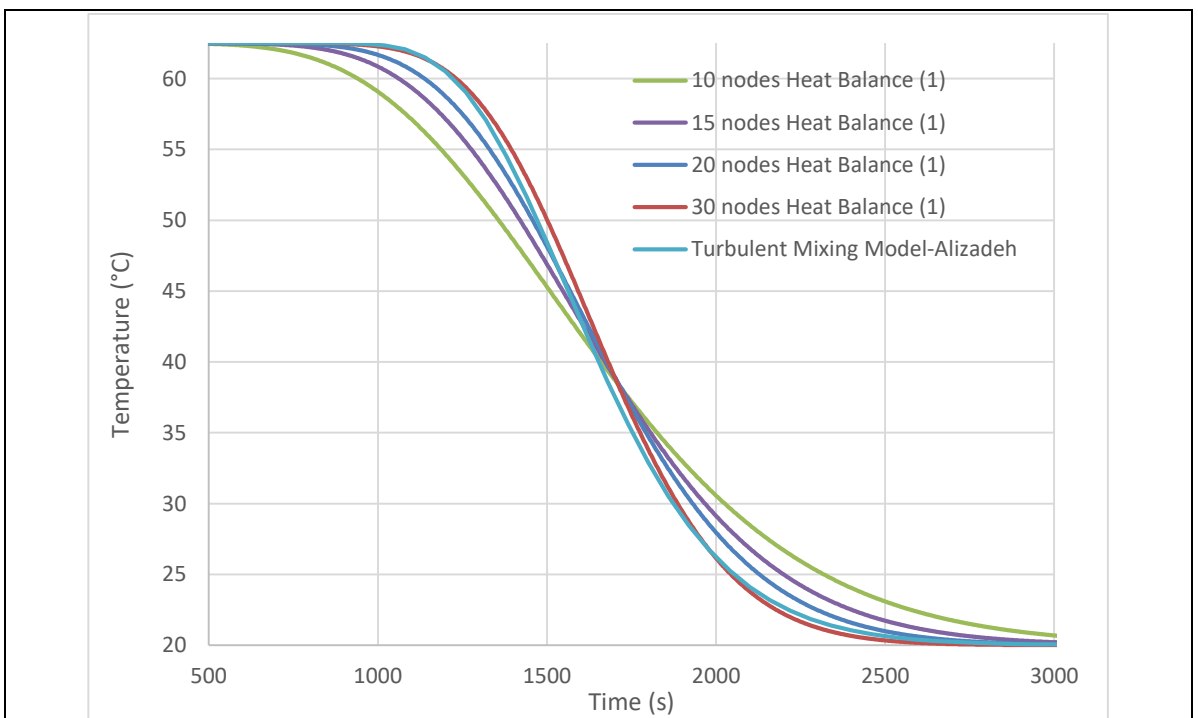


Fig. 5 Comparison of simulated results obtained with the heat balance (1) with Alizadeh's model 15 layers [11]. Only the temperature of the top layer is plotted. Test realised with flow-rate of 11l.min<sup>-1</sup> and a tank of 300l.

The heat balance of the tank was simultaneously studied during the test case. It appeared that less than 0.05% of the energy content of the tank was missing at the output after a full draw-off. If this issue remains mostly unexplained, a part of the reason can reside in the use of a parametric model for the tank and the associated approximation of calculation made by the software.

### 3.3 HEAT EXCHANGER

Heat exchangers transfer energy between the three loops of the system. One links solar collectors to the solar heat storage and the other links the solar heat storage to the load tank. Counter-flow plate heat exchangers are commonly selected for domestic and commercial building use; they maximise LMTD.

In the case of the system studied, neither the outlet temperatures nor the heat transfers between fluids are known. Specifying instead the *Number of Transfer Units* (NTUs) allows us to override these issues [37]. The first step of calculation consists in estimating the maximum heat transfer possible  $Q_{max}$  between the two fluids consistent with the principle of energy conservation and for specified inlet temperatures (2). Then the NTU number (3) is calculated using the properties of both fluids and heat exchanger. A number  $Z$  (4) is also computed to determine the configuration in which the efficiency has to be calculated. Finally, the efficiency of the heat exchanger is given by (5) or (6), the heat transfer can therefore be estimated by multiplying the value found in (2) by the one found in (5) or (6). Heat losses inside of the heat exchangers have been neglected in this project.

$$Q_{max} = C_{min} \cdot (T_{hot,in} - T_{cold,in}) \quad (2)$$

$$NTU = \frac{A_{ex} \cdot U_{ex}}{C_{min}} \quad (3)$$

$$Z = \frac{C_{min}}{C_{max}} \quad (4)$$

$$if Z > 1 : \eta = \frac{1 - \exp(-NTU \cdot (1 + Z))}{1 - Z \cdot \exp(-NTU \cdot (1 - Z))} \quad (5)$$

$$if Z = 1 : \eta = \frac{NTU}{1 + NTU} \quad (6)$$

The NTU method is implemented in *Simulink* with *User Defined Function*, the code embedded in these blocks is available in Appendix C.

The convective heat transfer coefficient of most of fluids, including water and ethylene glycol, changes with temperature and velocity of the flow. Thus  $U$  the *Global Heat Transfer Coefficient* (GHTC) of the heat exchanger (inverse of the thermal resistance) also varies with these parameters. The time allocated for the project did not give us the opportunity to do research and implementation the variation of these coefficients. For convenience, they are then considered constant.

The model was tested over the range of flow-rates likely to be found in the system, from 0 to 0.5 l.s<sup>-1</sup>, the conservation of energy was respected in any case.

Two plate heat exchangers are tested in the model to assess their influence on the efficiency of the system. Their characteristics are given in Table 1.

Table 1 Characteristics of the two heat exchangers used in the simulations, *Northern Lights* [38]

	Heat transfer area (m <sup>2</sup> )	GHTC (W.m <sup>-2</sup> .K <sup>-1</sup> )
Heat exchanger 1	0.322	2280
Heat exchanger 2	0.672	2180

### 3.4 SOLAR PANEL – CONTROL OF THE SOLAR LOOP

#### ➤ *Model of solar panels*

Solar panels are modelled with the Hottel-Whillier-Bliss theory [39-40]. The solar heat addition (7) is function of the efficiency of the collector (8), this last being itself dependant on both operating conditions (9) (average temperature of the panel, solar irradiation and ambient temperature) and intrinsic parameters of the solar panel (design, insulation, type of heat exchange fluid...).

$$Q = \eta \cdot A_c \cdot G \quad (7)$$

$$\eta = \eta_0 - a_1 \cdot T_m^* - a_2 \cdot G \cdot T_m^{*2} \quad (8)$$

$$T_m^* = \frac{T_m - T_a}{G} \quad (9)$$

Where  $\eta$  is the collector efficiency,  $A_c$  is the projected area of the collector,  $G$  is solar irradiation, and  $T_m^*$  is a scaled temperature (units of K.m<sup>2</sup>.W<sup>-1</sup>).

The optical efficiency  $\eta_0$  (efficiency under standard conditions), coefficients  $a_1$  and  $a_2$  (coefficient of heat losses) are determined with the European standardized testing procedure defined in the norm EN12975 and known as the *Steady State Testing* [41]. The values used in this study are provided by the *Institut für Solartechnik* (SPF) [42], an official Swiss organisation assessing solar thermal related devices.

The SPF data apply to flat plates and evacuated tubes under wind-free conditions. In locations such as Bristol, windy conditions can result in a significant increase in unwanted forced convection heat losses from panels. The results obtained during simulations will therefore be interpreted and discussed carefully in regard of this issue.

The mass flow rate of heat exchange fluid delivered by the feeding pump to the panels is controlled electronically according to ref. [43].

$$\dot{m}_c = \frac{0.05}{60} \cdot \Delta T \cdot A_c \quad (10)$$

Where  $\dot{m}_c$  is mass flow rate in units of kg.min<sup>-1</sup>,  $\Delta T$  is the temperature difference specified in °C, and  $A_c$  is specified in m<sup>2</sup>.

Using a variable instead of constant flow rate allows one to decrease the energy consumed by the feeding pump while marginally affecting the quantity of solar energy harvested. The control is based on the difference of temperature of the heat exchange fluid at the inlet  $T_1$  and at the outlet  $T_2$  (see Fig. 2) of the collector (SC) rather than directly on the level of solar irradiation, as it results in a more stable functioning of the system, especially on cloudy days where appreciable, rapid changes in  $G$  are possible.

To prevent winter freezing of the heat transfer fluid, an aqueous solution of 33% by mass ethylene-glycol is employed (freezing temperature = -17°C and boiling temperature = 104.4°C [44-45]).

The model is implemented in *Simulink* by the use of a *User Defined Function* embedding a Matlab code (see Appendix D). The module was able to reproduce the curves of peak power and efficiency at 1000 W.m<sup>-2</sup> given by SPF.ch for the two different collectors. Tests were also performed for different (constant) values of solar irradiation and results shown the expected tendency of a decrease of the efficiency with the decrease in irradiation and increase in temperature.

### ➤ **Control of the solar loop**

The solar loop is comprised from the solar collectors (SC), the solar heat storage tank (ST), the heat exchanger (HX1) and the pumps P1 and P2. The controller should turn off the loop (turn off P1 and P2) if freezing or boiling points of the heat transfer fluid are approached

The controller should verify that the temperature  $T_2$  of the heat transfer fluid at the outlet of the solar collector (SC) is higher than the temperature  $T_3$  at the bottom of the storage tank (ST), to ensure that the fluid will heat the content of the storage tank (ST) and not reversely. If not, the pump P1 will continue to feed collectors until the temperature of the heat transfer fluid reaches an adequate temperature or until the efficiency of the panel drops below zero (i.e. when operating conditions do not allow the harvesting of energy).

Additionally, the solar loop is controlled by a thermostat which monitors the temperature  $T_4$ . Its purpose is to turn on or off the feeding pump P1 of the collectors if the tank is fully heated. The thermostat follows the rules given in (11-13).

$$\text{If } T_4 > 75^\circ\text{C}, \text{ solar loop} = \text{off} \quad (11)$$

$$\text{If } 70^\circ\text{C} < T_4 < 75^\circ \begin{cases} Q_{\text{previous}} = 0, \text{ solar loop} = \text{off} \\ Q_{\text{previous}} > 0, \text{ solar loop} = \text{on} \end{cases} \quad (12)$$

$$\text{If } T_4 < 70^\circ\text{C}, \text{ solar loop} = \text{on} \quad (13)$$

The implementation of the logic of the solar heating controller is shown in Appendix D.

## 3.5 GAS BOILER – CONTROL OF THE HEATING LOOP

### ➤ **Model of the gas boiler**

The modelled gas boiler provides a constant heat flow to water when turned on. Its rated power supply is 61kW, subject to a boiler efficiency of 80% irrespective of season (according to the Sustainability Service, University of Bristol). In *Simulink* the outlet temperature of the boiler is calculated by adapting the steady flow energy equation to a pure liquid experiencing minimal changes in kinetic and potential energy, and with minimal pumping power.

$$T_{\text{out}} = T_{\text{in}} + \frac{Q_{\text{boiler}}}{c \cdot \dot{m}} \quad (14)$$

The flow-rate of water passing through the boilers, is set at 12 l.min<sup>-1</sup> in conformity with boilers of comparable power. See Appendix E for the Matlab code.

### ➤ **Control of the heating loop**

In both the current configuration of the system (Fig. 1) and the proposed solar-assisted version (Fig. 2), heating is switched on/off using a thermostat monitoring the temperature of the colder bottom layer of the load tank  $T_3$  and the most recently estimated heat output  $Q_{previous}$ . The rules are:

$$\text{If } T_{in} > 65^\circ\text{C}, \text{heating} = \text{off} \quad (15)$$

$$\text{If } 60^\circ\text{C} < T_{in} < 65^\circ \begin{cases} Q_{previous} = 0, \text{heating} = \text{off} \\ Q_{previous} > 0, \text{heating} = \text{on} \end{cases} \quad (16)$$

$$\text{If } T_{in} < 60^\circ\text{C}, \text{heating} = \text{on} \quad (17)$$

In the current configuration the gas boiler is the only source of heat for the load tank. In the proposed configuration the gas boiler is one part of the heating loop comprised from the solar heat storage tank (ST), the load tank (LT x2) and one heat exchanger (HX2). Heat can be provided by the solar heat storage tank, the gas boiler or by both of them at the same time. A proper management of these heating devices is likely to increase the proportion of energy brought to the system by the renewable source. Thus a controller including two additional rules is added. The two rules are based on the difference of temperature between the top of the solar storage tank (ST)  $T_4$  and the bottom of the load tank (LT)  $T_7$ .

The first rule decides if the heating system can extract energy from the solar heat storage tank (ST)

$$\text{If } T_5 > T_7, \text{pump } 3 = \text{on}, \text{else pump } 3 = \text{off} (\text{Fig. } 2) \quad (18)$$

This condition prevents the unwanted reverse case were the load tank would heat the solar storage tank.

The second rule completes the first one in the case where the system is able to use the solar storage tank and the boiler (B). In this situation a threshold ( $T_{ref}$ ) on the difference of temperature is defined:

$$\text{If } T_5 - T_7 > T_{ref}, \text{pump } 3 = \text{on and } B = \text{off} (\text{Fig. } 2) \quad (19)$$

$$\text{If } T_5 - T_7 < T_{ref} \text{ and } T_5 > T_7, \text{pump } 3 = \text{on and } B = \text{on} (\text{Fig. } 2) \quad (20)$$

$$\text{If } T_5 - T_7 < T_{ref} \text{ and } T_5 \leq T_7, \text{pump } 3 = \text{off and } B = \text{on} (\text{Fig. } 2) \quad (21)$$

The smaller the threshold the higher the quantity of energy provided by the solar storage, and therefore the higher the solar fraction is likely to be. Validation tests leads to the conclusion than an activation threshold set at  $20^\circ\text{C}$  allows to transfer the maximum amount of energy while maintaining acceptable heating times.

The logic implemented in the controller, which repeats the controller at each step of simulation, is summarised on Fig. 6. Appendix E shows how the logic is implemented in Simulink.

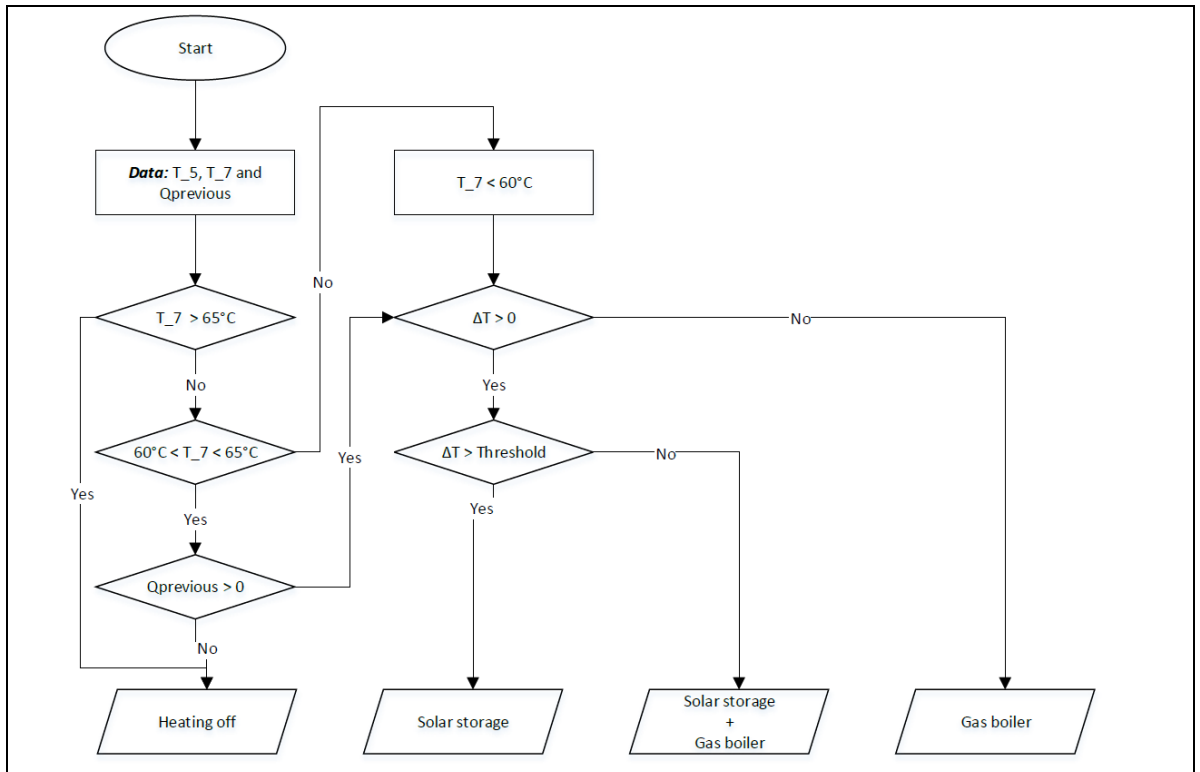


Fig. 6 Diagram of control of the heating process as a function of the temperature at the bottom of the load tank  $T_7$ , the temperature at the top of the solar tank  $T_5$  and the output of the heating system during the previous step of simulation  $Q_{previous}$ . Operation repeated at each step of simulation.

### 3.6 PIPEWORK

In a hot water distribution system, pipes introduce an appreciable time delay depending on their length and on the velocity of fluid inside, and are an important source of heat and head losses. Thus they have a direct impact on the quantity of energy required to heat water. Ferguson-Brown were unable to characterise the pipework of Baddock Hall.

The temperature of the pipe and the fluid it contains depends on the distance to the input of the fluid and on the time. To study the heat flow, both pipe and fluid have to be divided into layers on which a heat balance is applied. For each element the balance takes into account the effect of forced convection, conduction and heat losses.

Test cases prior to the implementation in the model have highlighted the numerical diffusion issue inherent to that type of parametric Eulerian representation. The model predicts an increase in temperature at the output of the pipe before the moment at which the fluid should theoretically arrive. Increasing the number of nodes (or diminishing the size of layers) results in a reduction of the numerical diffusion. However, time step and size of layers are linked by the Fourier and Courant criterions which define the domain of stability of the solution. Consequently, a decrease in the size of layers implies a decrease in the time step.

The QUICK scheme [46] was implemented to try reducing the influence of numerical diffusion for the same number of nodes, but besides adding overshoot with no physical explanation (purely mathematical issue), the number of nodes required remains high to get satisfactory results, see Fig. 7.

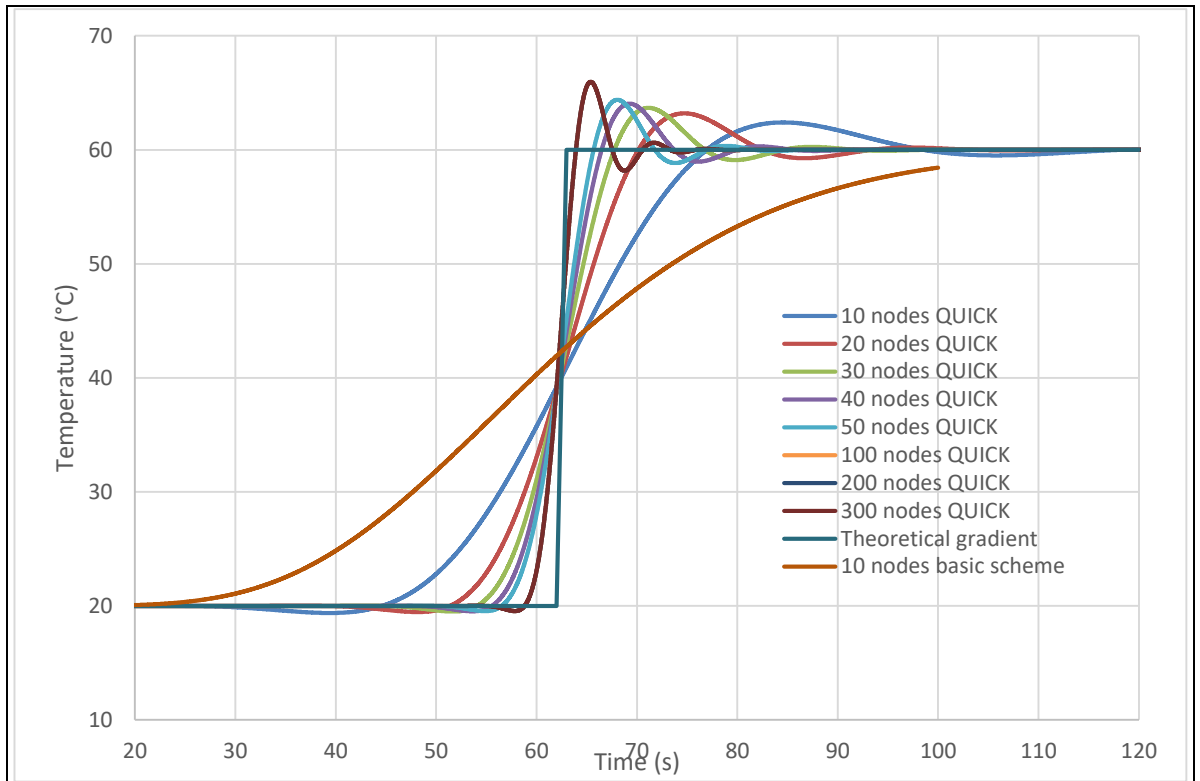


Fig. 7 Temperature evolution at the outlet of the pipe obtained during test cases on a 36m long pipe and a flow of velocity  $0.58\text{m}\cdot\text{s}^{-1}$ . The QUICK scheme improves the result in time for high number of nodes but introduces overshoot.

To comply with Taylor theory on diffusion of matter in flows [47], more than  $10^4$  layers and a time step below  $10^{-3}$  s are required. These values are totally unsuitable for simulations over 30 days (more than 2.5 billion of steps resulting in CPU time over 2 hours) with the available computer. This issue combined with the absence of any data relative to the pipework at Baddock Hall resulted in the choice to neglect pipes in the model.

### 3.7 INPUTS AND PARAMETERS OF SIMULATION

#### ➤ Demand pattern of Baddock Hall

A demand pattern was defined by Knight, N. [48] in a previous study of the electric hot water heating system of Baddock Hall and reportedly gave coherent results when compared to measurements on site. The definition of this profile was based on Ferguson-Brown audit which, according to the measurements they made, indicates four peaks of consumption per day, a maximum draw-off rate of 250l over 30 minutes, and a total daily hot water consumption of  $1.7\text{ m}^3$  for 45 people. A correlation between their advice and a set of measurements provided by the *Sustainability Service* of the University of Bristol was made to enhance the profile. The maximum flow rate during peaks was estimated with the “fixture unit” method in a case where only showers are used.

A scaling factor was introduced by Knight, N. to take into account overloads and variations of the demand, bringing the total volume of hot water consumed to 2400l per day for 45 people. After a validation test, the current gas boiler installation appeared to be totally unsuitable for such a loading with temperature of water at the output of the tank dropping below  $20^\circ\text{C}$  during each peak. The decision was made to reduce by 25% the demand so as to meet the figures defined by Ferguson-Brown experts. The total load used in this project is then 1800l per day, 5.8% greater than the F-B value.

As explained in part 3-1, the gas heating system of Baddock is comprised from two tanks and two gas boilers working in parallel, then each of these tanks provides half the daily load, i.e. 900l. The demand seen by one tank is shown on Fig.8.

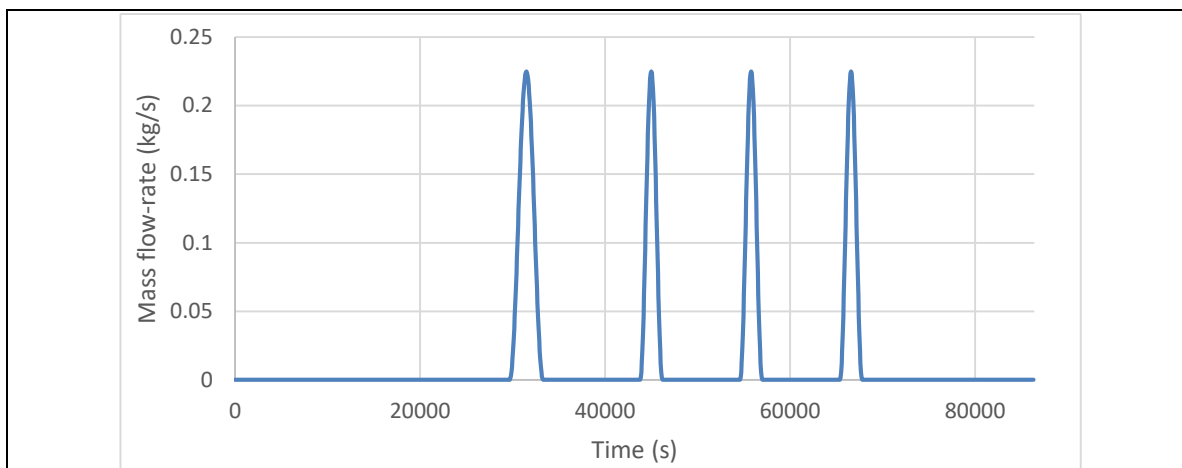


Fig. 8 Profile of hot water demand seen by one unit of the installation of Baddock Hall, defined by Knight, N.

#### ➤ *Weather data*

The efficiency of solar collectors essentially depends on ambient temperature and solar irradiation, the use of an appropriate set of data has therefore a direct impact on the reliability of the outputs of the model. Baddock Hall being located in Bristol, England, two sources of information were accessible:

- the SOLAREC-PVGIS, an official weather database of the European Union [49].
- a weather station based in Filton, distant of 6km kilometres from Bristol [50].

The SOLAREC-PVGIS database provides solar irradiation and ambient temperature for different locations, months, orientations and tilts of solar panel. Supplying the previous parameters yields a smoothed diurnal profile for both solar irradiation and ambient temperature. However, no information on the amplitude of variation across a day are provided. This drawback can make the use of such a dataset questionable when it comes to estimate the energy likely to be harvested by a solar collector. For this reason, SOLAREC-PVGIS data were only used for test cases.

The weather station of Filton measures continuously various solar and atmospheric parameters and gives access to 10 years of archives. Contrary to the SOLAREC-PVGIS, data cannot be interrogated to account for the orientation and tilt of the panel, nonetheless the dataset shows the important influence of cloud covering on solar irradiation during a day and presents a variation in the profile from one day to another. With regards to the data from the station (it has not been possible to know what type of apparatus was used), nonetheless this was more realistic than repeating the same profile for every day of a month. Fig. 9 (a) and (b) illustrate the differences between SOLAREC-PGVIS data and measurements made by the weather station in Filton.

In any case (weather station or SOLAREC-PVGIS) the total solar irradiation (sum of the direct, diffuse and reflected irradiations) is used.

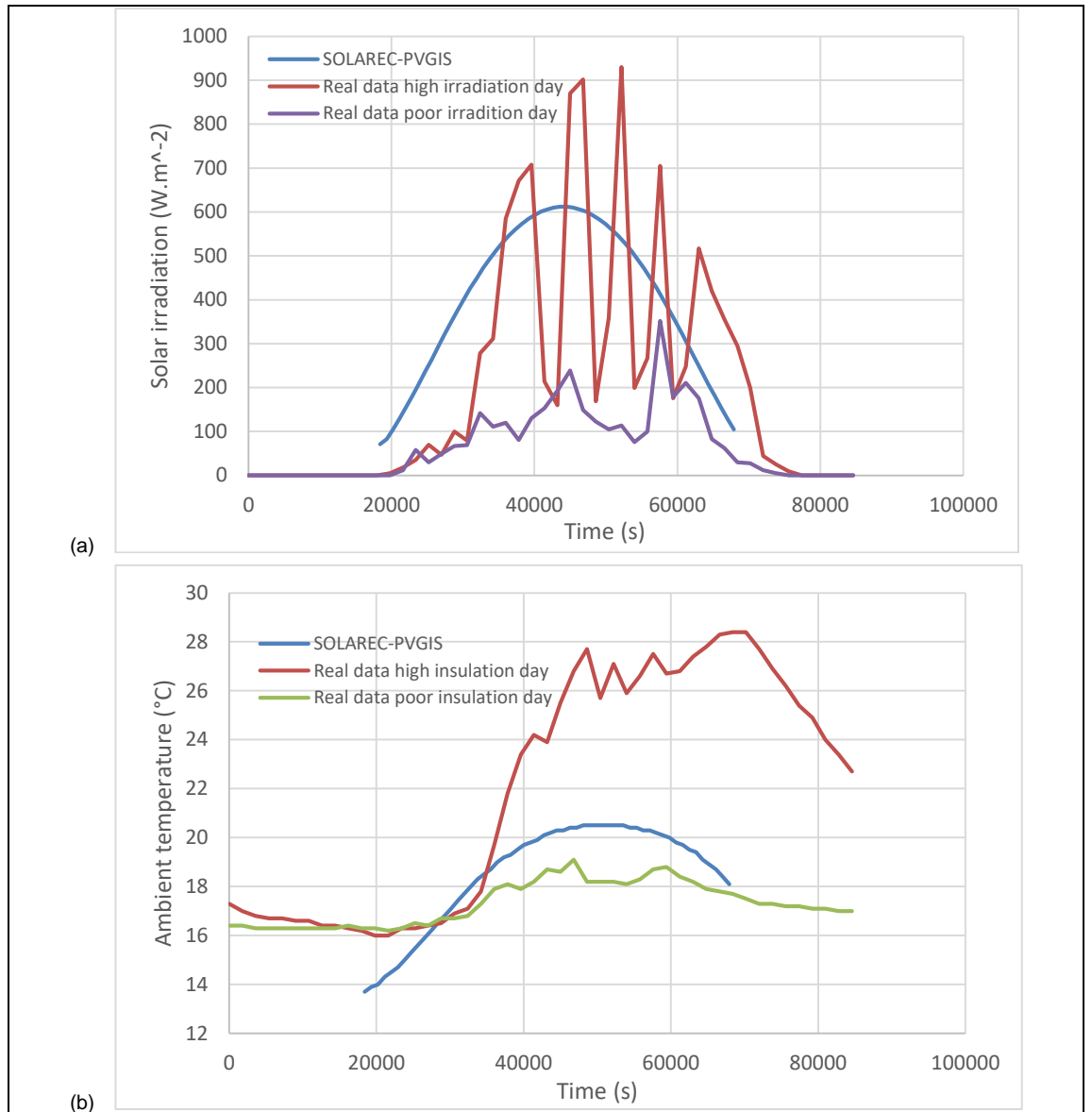


Fig. 9 Comparison of (a) solar irradiation and (b) ambient temperature between the smoothed values of the SOLAREC-PVGIS and the real measurements made in Filton the 16<sup>th</sup> (low irradiation) and 18<sup>th</sup> (high irradiation) of July 2016.

➤ *Investigation on time step*

The model of stratification requires a careful analysis of the influence of the time-step. The time step was subject to the Fourier criterion for stability given in (22).

$$\frac{\lambda}{\rho \cdot c} \cdot \frac{\Delta t}{(\Delta x)^2} \leq 0.5 \quad (22)$$

and to the Courant criterion for convergence of the solver (23).

$$u \cdot \frac{\Delta t}{\Delta x} < 1 \quad (23)$$

Where  $u$  is the velocity of the flow in the tank,  $\Delta t$  the time step and  $\Delta x$  the height of a layer. In the case of the model developed here, the time step theoretically limited to 85s by Courant. However, the convergence of the results as a function of the value of the time step in the acceptable range provided by both criteria has to be investigated.

The study of the impact of the time-step was performed using the SOLAREC-PVGIS profile for London in July (shown in Fig. 9) and the demand profile of Knight, N.

(shown in part 3-7). The simulation was done over 10 days (simulated time). Two parameters were considered: the energy content, and the temperature difference between the top and the bottom of the tank. The following configuration of solar pre-heating system was used for the test:

- Solar heat storage of 400l capacity
- 16 m<sup>2</sup> of solar thermal collectors Riello CSAO 25R
- Heat exchangers with U.A = 1466 W.K<sup>-1</sup>

Initially the two tanks were considered having their entire content at 20°C.

A time-step greater than 45s caused unrealistic predictions of temperature and consequently the model malfunctioned. During periods of high insolation (typically middle of the day) the liquid in the panel exceeds its boiling point, leading to an irretrievable shutdown of the solar loop. The test was repeated for the following time steps: 40s, 30s, 20s, 10s, 5s, 4s, 3s, 2s, and 1s, with the ode1 (Euler) solver of Simulink.

The day-to-day changes of both energy content ( $E(k) - E(k-1)$ ) and temperature difference between the top and the bottom ( $[T_4(k)-T_3(k)] - [T_4(k-1)-T_3(k-1)]$ ), where  $k$  is the day number, of the heat storage tank are studied. The system will converge from arbitrary initial conditions to a cyclic steady state. During the first days the difference, one expects the differences to be non-zero the time to reach convergence. Also the time to converge and the converging value is expected to vary with the size of the time step. Results are plotted on Fig. 10 (a) and (b)

The energy content and the temperature gradient converge after the third day for time steps above 2s, below this value the convergence is almost immediate. Moreover, it can be observed that variations of up to 7% are reached from one day to another during the first 3 days above 2s, while less than 0.2% of difference is obtained below this threshold. Therefore, choosing a time-step larger than 2s is susceptible to affect the output of simulations.

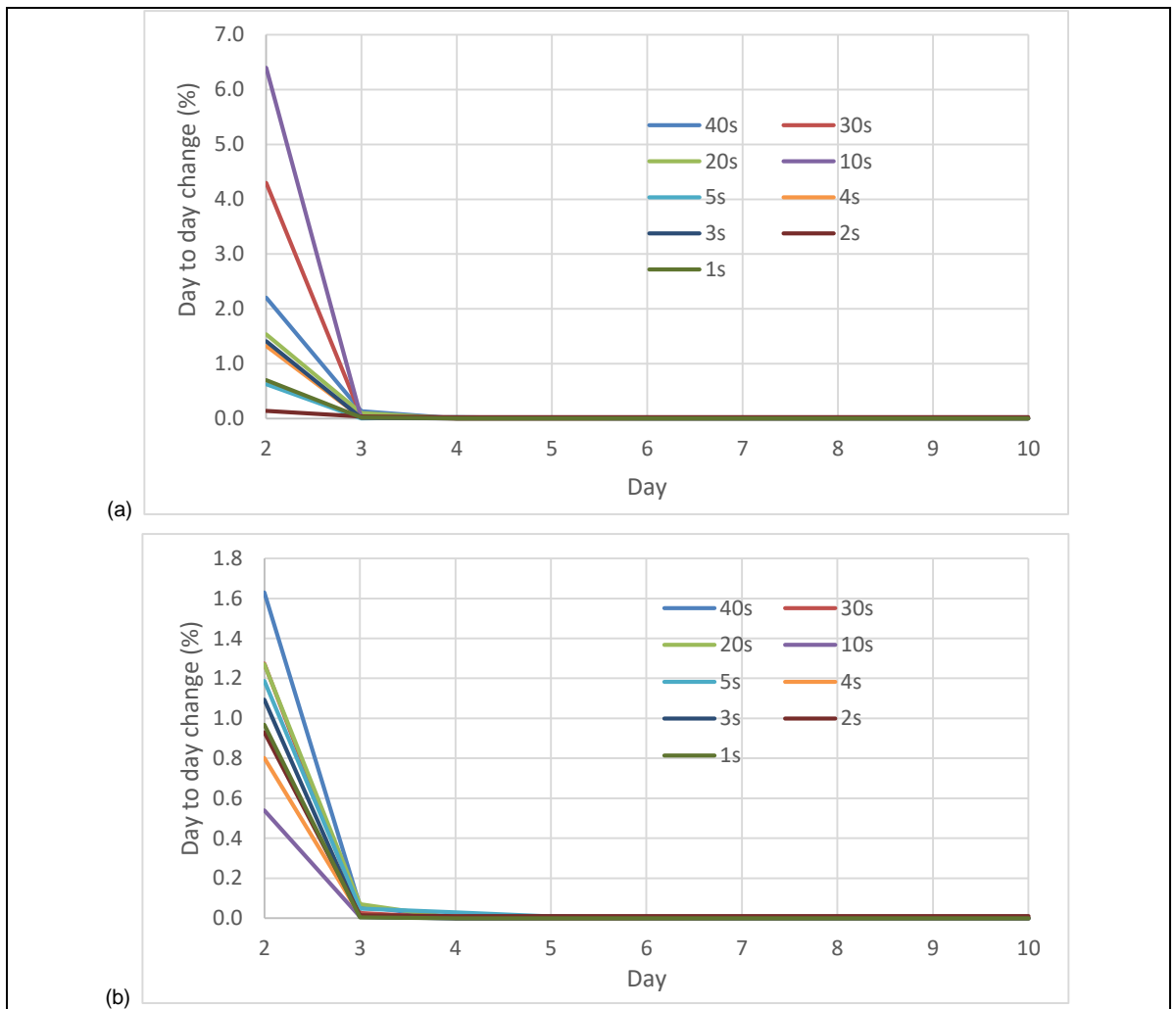


Fig. 10 (a) Convergence in day to day change of the temperature difference between the top and the bottom of the tank and (b) convergence in error of the energy content of tank

As a final check, the convergence of the error between successive values of the time step for both studied parameters after 10 days is shown on Fig. 11. For time steps exceeding 2s, outputs are subject to variation of more than 5%. Smaller time steps resulted in more accurate simulations. However, selecting a time step below 2s leads simulation time above 30min, forcing the value of 2s.

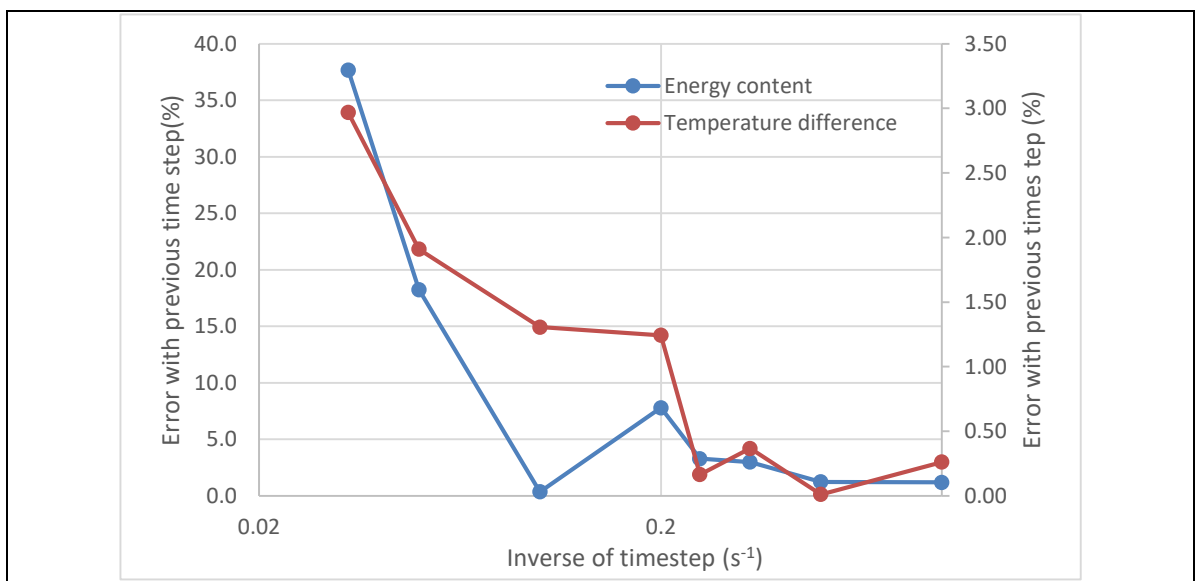


Fig. 11 Convergence in error between successive values of the time step for both energy content and temperature difference.

➤ *Estimation of the initial gradient of temperature in tanks*

The initial gradient of temperature in the solar heat storage tank and in the load tank (at the beginning of the simulation) is primarily unknown.

It appears that despite the absence of any initial gradient in both tanks, a steady state is reached almost after the first day (using a time step of 2s). In the case of the load tank, heated by both the solar heat storage and the gas boiler, the gradient at the end of the day (i.e. at 0:00) corresponds to a tank fully heated and cooling slowly under the effect of heat losses to the ambient. To assess the influence of the use of the solar loops in the heating process on the gradient of temperature at the end of the day, a second simulation was performed with the model of the current installation of Baddock Hall. When compared, the two gradients obtained were close and the difference between the extreme temperatures (top and bottom of the tank) was below 2%, value which was considered acceptable. These values being in a range of 0.5°C and being affected by the diffuser it was decided that the average temperature of 64.78°C would be applied to all the layers of the load tank at the beginning of each simulation whatever the configuration or the month simulated.

The solar heat storage must be treated differently to the load tank because the temperature gradient depends on the weather conditions as well as energy at start of each day. To get the initial condition we repeated the profile of ambient temperature and solar irradiation of the first day during 4 days (simulated time) to get a converged value (see Fig. 12 (a)) for each configuration and each month simulated. This converging value was considered as the initial tank condition prior to using real world weather conditions as an input.

### 3.8 VALIDATION TEST OF THE SYSTEM

➤ *Validation of the energy consumption*

The first test compared the energy consumption predicted by the model to measurements made in the current Baddock Hall unit (see part 3-1). The consumption pattern inputted was the one defined in part 3-7. Simulation was made over one day with a time step of 2s.

The cumulative energy consumption over a daytime is shown on Fig. 10. The model predicts an energy consumption of 144 kWh (taking into account the efficiency of boilers) per day to meet the demand in hot water.

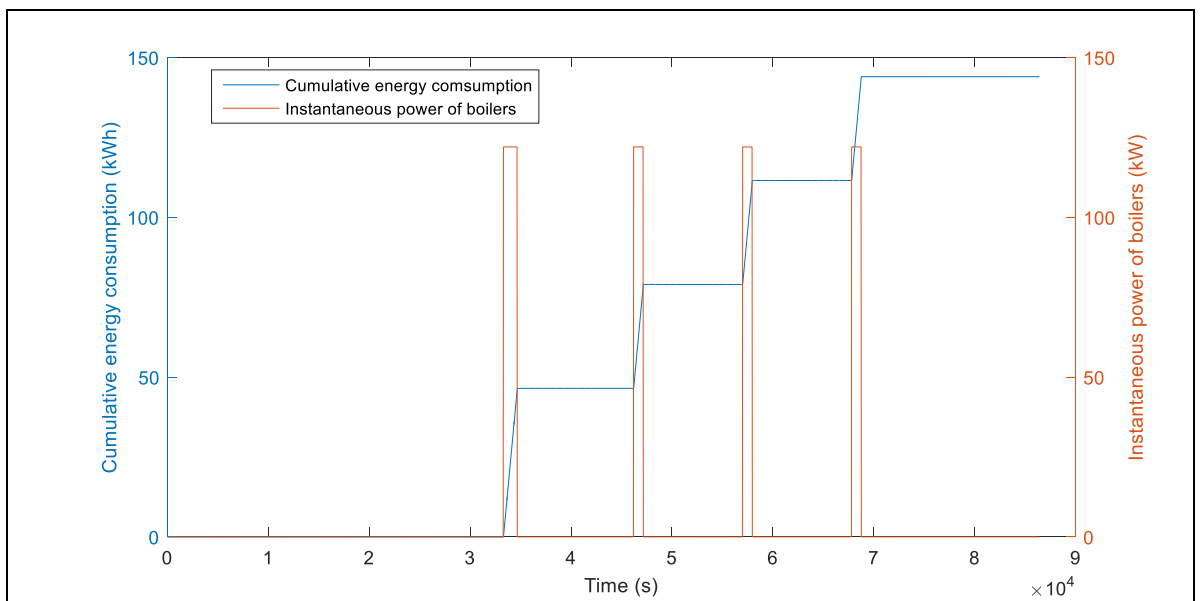


Fig. 12 Cumulative energy consumption and instantaneous power provided by the two boilers as a function of time, curves obtained with the *Simulink* model of the current gas heating Installation of Baddock Hall

The estimation of the real consumption of energy for water heating at Baddock Hall was made on the basis of data provided by the *Sustainability Service*. The measurements of consumption of three anonymised flats made in June 2016, equivalent to 5 to 6 people, were summed and multiplied by 3 to get an estimation of the consumption of 45 people. This method led to a maximum consumption over a day of 822.55 kWh, a minimum consumption of 103 kWh and an average of 387 kWh. This “real” average consumption would then be 270% greater than the prediction of the model. The model was verified and didn’t show any physics-related issues. However, deeper analysis of the data highlighted not only the presence of regular peaks of consumption but also an almost constant baseload. The baseload was most likely due to the use of central heating or to the secondary flow. An attempt to modify the dataset was performed by removing the baseload, estimated independently for each flat with an average. This led to a “modified” average consumption per day of 208 kWh per day, therefore still 43% bigger than predicted.

As no information on the way these measurements were made and what was effectively measured came in appropriate time to be included to the discussion, the modelling was kept unchanged for the rest of the project. The model including some assumptions such as the absence of a secondary flow and probably a more effective insulation than the current system (or reversely the current system might suffer from excessive heat losses through insulation) it is possible that the real consumption uniquely for hot water is between 144 kWh and 208 kWh. A more detailed study of Baddock Hall installations might grandly help sorting out the reasons of these discrepancies.

### 3.9 FINANCIAL MODEL

The financial assessment of the sixteen configurations of the solar pre-heating system employs the *Net Present Value* (NPV) of the system after an expected lifespan of 25 years of exploitation. It is assumed that the actual gas boiler installation is already amortised and able to last at least over the lifespan of the pre-heating system. The estimation of the savings is calculated by taking into account both capital and operational expenditures.

The capital cost stands for the purchase price of the components of the system and their cost of installation. The cost of each component, based on Alfa-Laval and Grundfos catalogues [51-52], is detailed in Appendix F. The cost of solar panels is divided between the cost of collector per m<sup>2</sup>, which depends on the type of panel, and the cost of installation which was estimated at £200 per m<sup>2</sup> [53]. Reference [53] state that this cost of installation allegedly also includes the cost of installation of all the other components associated to solar panels (pipework, tanks, heat exchangers, pumps). The capital cost of each version is given in Appendix G.

The operational expenditures are mostly due to maintenance costs and standing fees. The evolution of these costs over the next 25 years is difficult to predict, they are therefore kept constant in calculations. They are comprised from:

- £185 per year for the maintenance of gas boilers and the standing fees of gas supply, figure provided by the *Sustainability Service* of the University of Bristol.
- £18.m<sup>-2</sup> per year for the cleaning and maintenance of solar collectors [54].
- £100 every 5 years to replace the heat exchange fluid (ethylene glycol-water mix) of the solar circuit [53].

Potential failure of components is assumed to be covered by these annual and fixed fees.

The UK *Department for Energy and Climate Change* (DECC) publishes yearly its projections of fuel prices for the next 25 years. “Central” and “high” scenarios were extracted from the most recently available report ([55], 2015). Official figures are given in £/therm units and represent the purchasing price on the international market. To evaluate the price finally paid by the customer data are converted into kWh and increased by 40% to take into account the different fees and profits (excluding CCL) made by the state and companies [56], curves are plotted in Fig. 13.

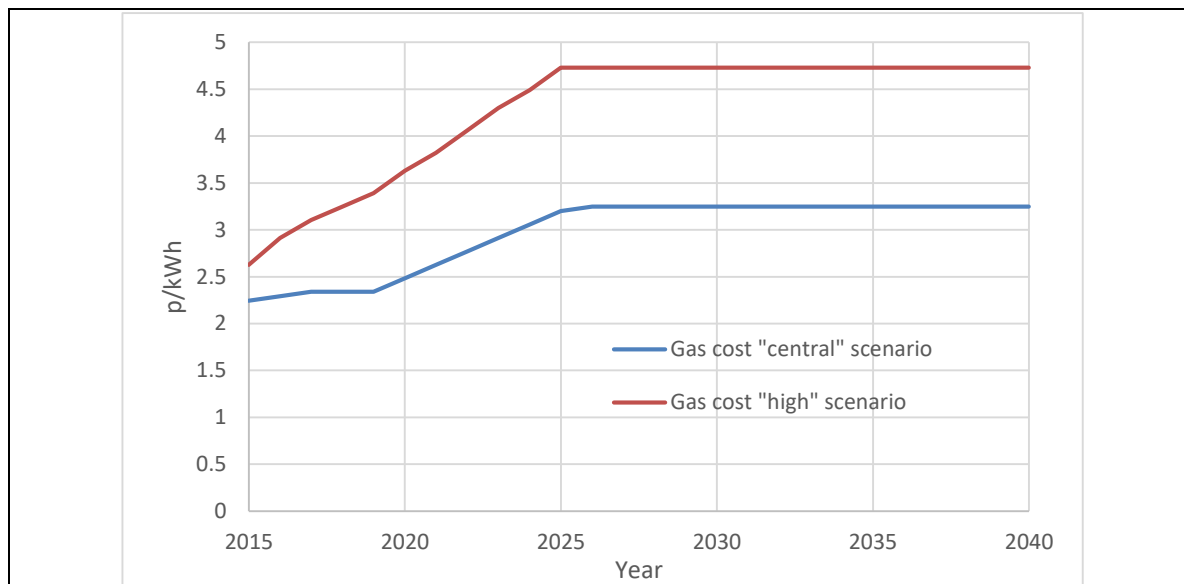


Fig. 13 2015 gas price (£) projections of DECC, increased by 40% for taxes and profits, “central” and “high” scenario.

The climate change levy (CCL) was assumed to increase by 5% per year including from 2019 to 2040. This is speculative because projections of CCL are presented only for up to four years in advance.

The *Renewable Heat Incentive* (RHI), which in England offers a payback of 19,74p per kWh of energy produced by the solar collectors during 7 years after the commissioning of the system, is also included in the assessment.

### 3.10 PLAN OF NUMERICAL EXPERIMENTS

To assess the impact of the components of the solar pre-heating system on the solar fraction and on the financial viability, 16 versions were tested. The parameters are the type of solar collector, the characteristics of the heat exchanger and the volume of the heat storage tank. For reminder, Solex BLUX is a collector with standard characteristics when the Riello CSAO 25R has top ones. Table 2 gives the details of each version.

Table 2 Configurations of the solar pre-heating system used for simulations

Solar collector	Surface of panel (m <sup>2</sup> )	Volume of solar heat storage (l)	Characteristics of heat exchangers (W.K <sup>-1</sup> )
Solex BLUX	16	320	733
Solex BLUX	16	320	1466
Riello CSAO 25R	16	320	733
Riello CSAO 25R	16	320	1466
Solex BLUX	16	400	733
Solex BLUX	16	400	1466
Riello CSAO 25R	16	400	733
Riello CSAO 25R	16	400	1466

Solex BLUx	20	400	733
Solex BLUx	20	400	1466
Riello CSAO 25R	20	400	733
Riello CSAO 25R	20	400	1466
Solex BLUx	20	500	733
Solex BLUx	20	500	1466
Riello CSAO 25R	20	500	733
Riello CSAO 25R	20	500	1466

During simulations the following outputs were stored:

- Temperature of layers inside of the load tank
- Temperature of layers inside of the solar heat storage tank
- Energy harvested by solar collectors
- Energy transferred from the heat exchange fluid to the heat storage tank
- Energy transferred from the heat storage tank to the load tank
- Energy consumed by the boiler (multiplied by 2)
- Heat losses of both tanks
- Efficiency of the solar collector
- Work done by pumps

The performances of each configuration in Table 2 were assessed over a year of simulated time. Because of the small time step of 2s, more than seven minutes (real time) are required to simulate a month (30 days) [CPU: Intel® Core™ i7-6700HQ CPU @ 2.60GHz]. This would have made the simulation of the full 12 months' operation of all 16 configurations exceed the time available for completing this thesis (12 x 16 x 6 = 1344 minutes = 22.4 hours). Hence the number of simulated months was reduced from 12 to 6. It was shown that the integration method (Newton-Cotes, Simpson, rectangular middle centred) had little impact on the error of approximation.

To keep the extremum of temperature and irradiation of the year the data of the following months were extracted from Filton weather station database (see part 3-7): January 2015, March 2016, May 2016, July 2016, September 2015, November 2014. Data are not from the same year essentially because the project was made in summer 2016; measurements of November 2015 presented a gap of several days, thus data of 2014 were used.

## 4 Results and discussions

### 4.1 SOLAR FRACTION AND IMPACT OF COMPONENTS

According to the plan of experiments six simulations are run for each of the sixteen versions of the system. The solar fraction was studied from two viewpoints: firstly, the monthly and annual values and secondly the influence of the characteristics of each component.

#### 4.1.1 Analysis of the solar fraction (monthly and annual)

The monthly solar fractions obtained by simulation for the 16 configurations of the solar pre-heating system are shown on Fig. 14.

The peak of efficiency of the solar system is clearly reached between April and August. In May, where the model predicts the maximal efficiency, monthly solar fractions reach values from 24% for the least efficient configuration to 36% for the most efficient one. These figures are in the range or above the estimation of SPF for solar pre-heating (25%), discrepancies are due to the different components embedded in systems.

The solar fraction increases markedly in spring and decreases markedly in Autumn; variations of more than 10% from one month to another are predicted. At the same time the difference between configuration becomes evident: it flattens in autumn and grows in spring. Still, the pre-heating can provide an appreciable amount of energy, which (depending on the system configuration) remains in the range of 10 to 17% minimum in March.

In winter however, the monthly solar fraction drops below 5% and the differences between solutions are in a range of 2.3%, five times smaller than in summer. The difference between January's results and November's ones is weak. In any case, the solar pre-heating system will provide a small, if not negligible, part of energy needed during these months. These results are coherent with the estimated evolution of solar insolation in Bristol given by the *Solar Electricity Handbook 2016* [57]. The model gives then coherent results relatively to what could have been expected.

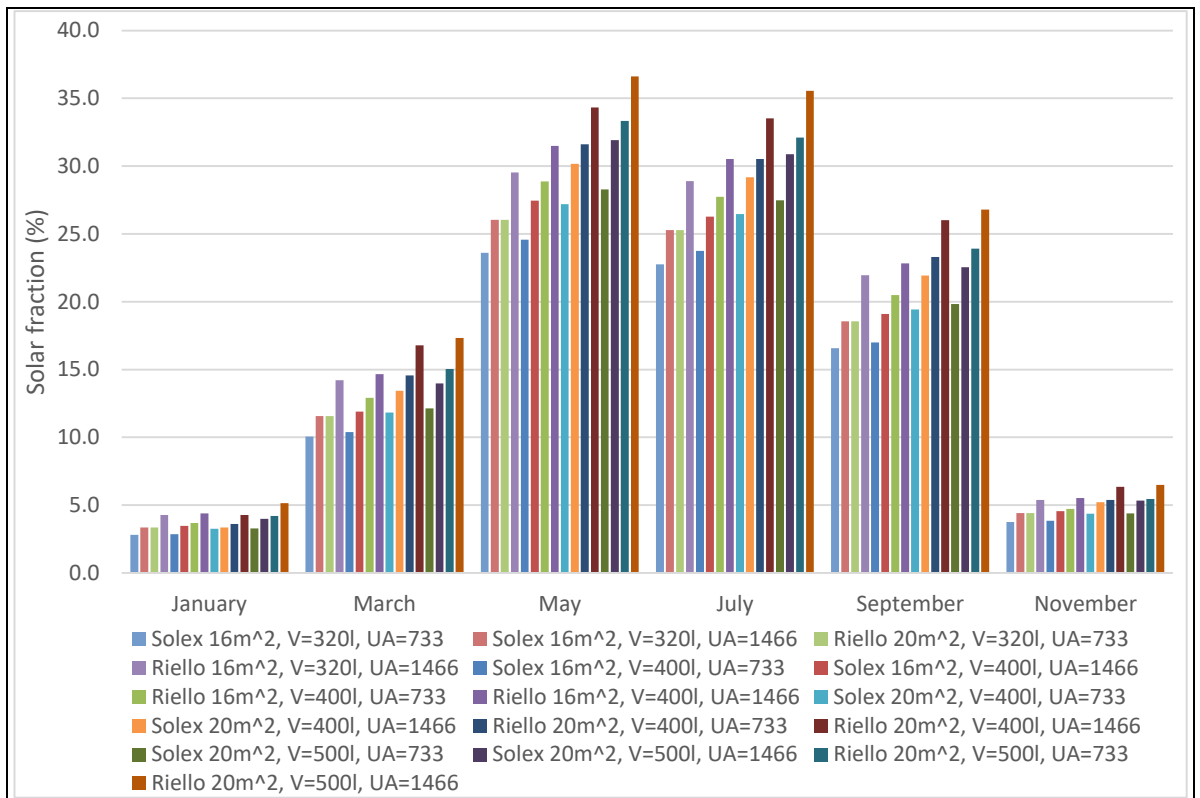


Fig. 14 Monthly solar fraction obtained for the 16 configurations of the solar pre-heating system over the six months simulated.

To assess the global performance of the systems over the twelve months of a year the annual solar fraction is calculated by rectangular integration over the six months simulated (Fig. 15).

In any case, the annual solar fraction is almost equal to 50% of the solar fraction measured in May. This confirms the observation made on Fig. 14 that the solar system will work efficiently the six months' period between April and September. The contribution to energy consumption during the rest of the year is significantly lower, and financial returns will be poor: seasonality is the main drawback of solar energy.

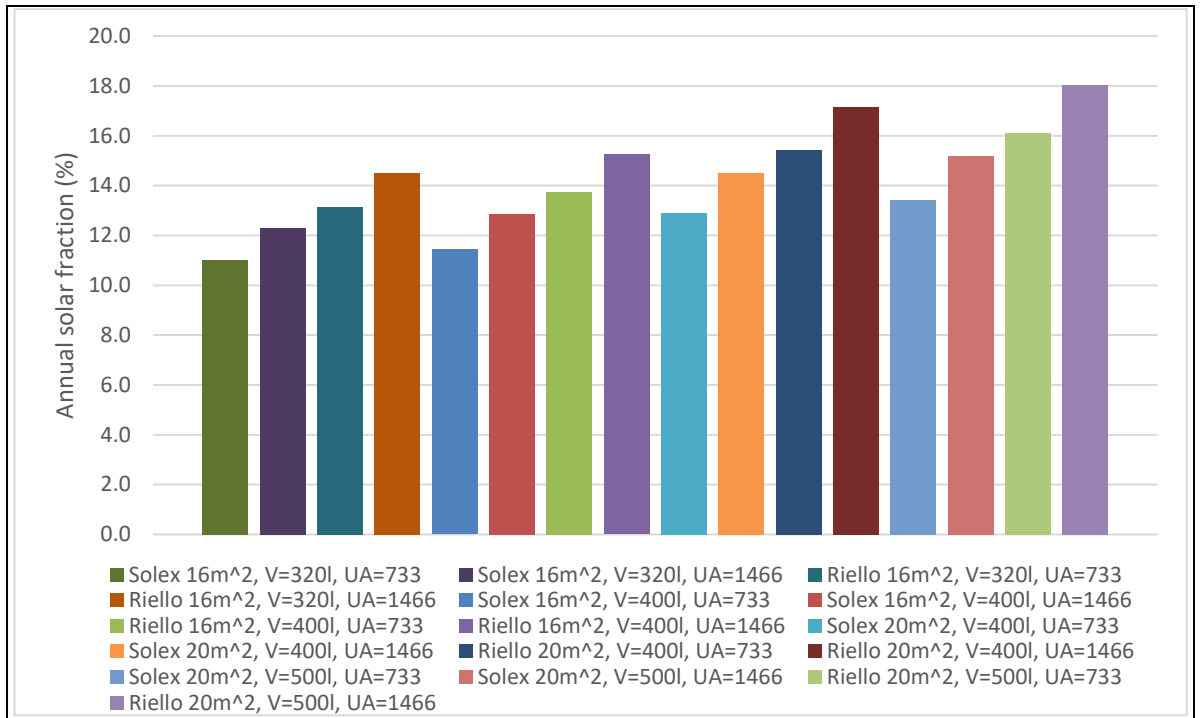


Fig. 15 Annual solar fraction estimated by regression for the 16 configurations of the solar pre-heating system.

The variability of the solar fraction depends on season but also on the components embedded in the system. The following describes and explain the impact of the different components.

#### 4.1.2 Effect of heat exchangers

Fig. 14 and Fig. 15 make obvious that doubling the area or heat transfer coefficient (that is, U.A) of the two heat exchangers (HX1 and HX2) yields a noticeable increase in the solar fraction, 1% to 2% annually and from 2% to up to 5% monthly in the period of high insolation (April to September).

Larger heat exchangers ( $U.A = 1466 \text{ W.K}^{-1}$ ) increase the quantity of heat transferred between fluids, consequently the outlet temperature of hot and cold fluids are respectively cooler and hotter than with a small heat exchanger ( $733 \text{ W.K}^{-1}$ ). The benefits of such a change are that:

- The working liquid returns to the collector at a lower temperature, the average temperature of the collector is then decreased and higher collector efficiencies are obtained. The difference in pump work illustrates this improvement, see Fig. 16. Solar collectors work longer every day, or at a higher flow-rate (or both combined) and this all year long. A clear increase in pump work happens during the cold period, showing that collectors are now more suited to harvest heat at low levels of ambient temperature and solar irradiation.

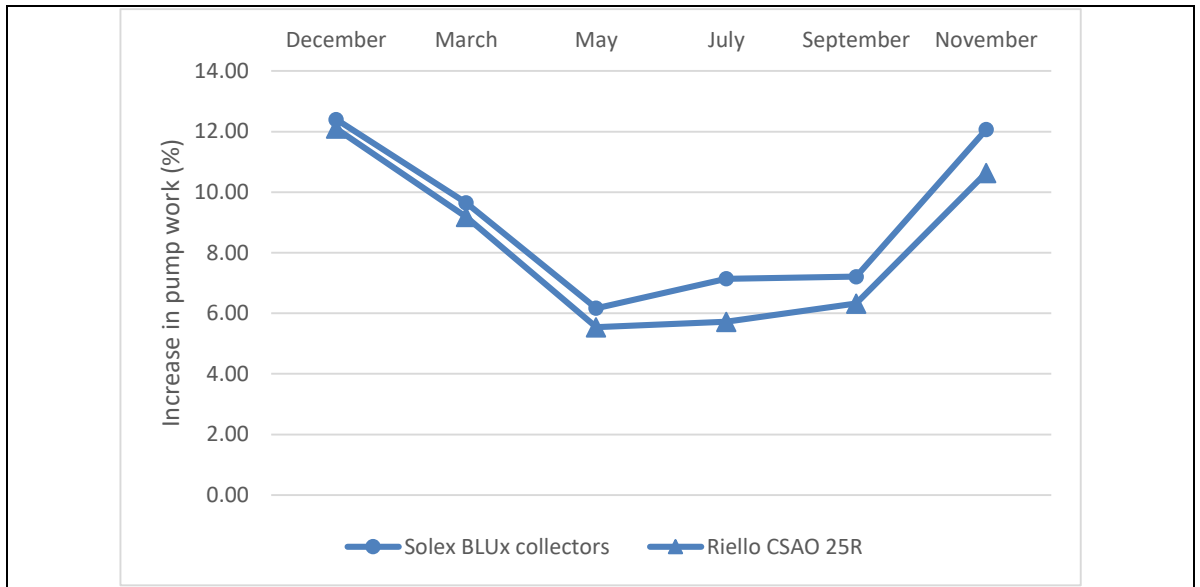


Fig. 16 Average increase in the work of the feeding pump P1 of solar collectors when the capacity of heat exchangers (HX1) is raised from 733W/K to 1466W/K, calculated for the Riello and Solex collectors.

- The speed of pre-heat of the load tank is decreased as the rate of heat exchanged is more important. Therefore, the work required by the three pumps feeding the heat exchanger between the heat storage tank to the load tank (P3 and P4 x2, see Fig. 2) is significantly reduced as shown on Fig. 17. Evidently the reduction in pump work is more important during the summer period as more energy is available to be transferred.

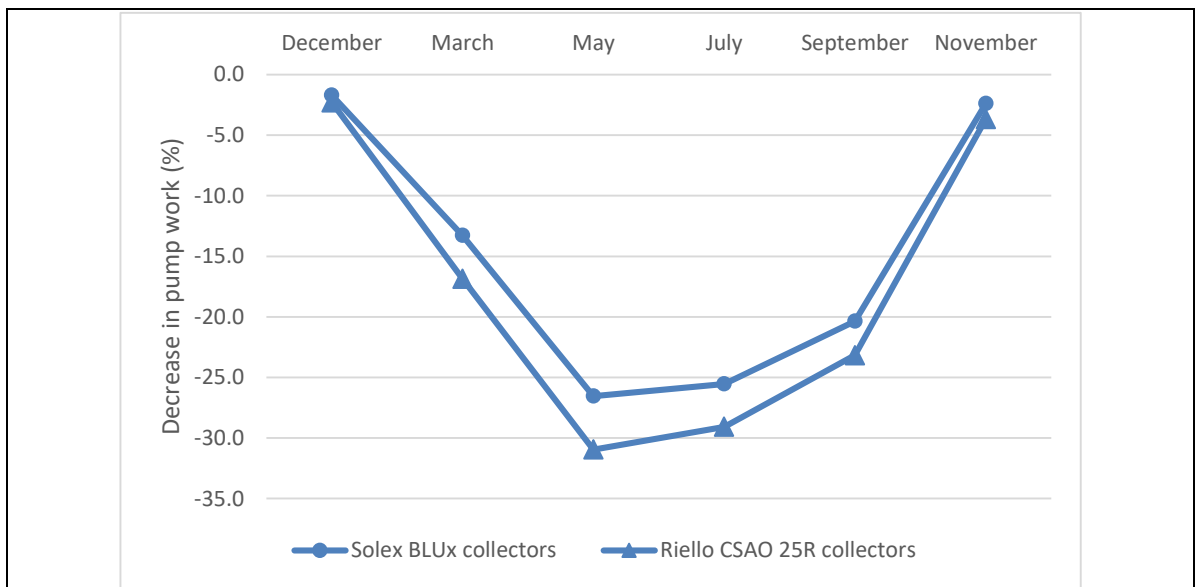


Fig. 17 Average reduction of the work provided by the three pumps feeding the heat exchanger (P3) between the heat storage and the load tank (P4 x2) when the capacity of heat exchangers (HX1 and HX2) is raised from 733W/K to 1466W/K, calculated for Riello and Solex collectors.

- The capability to transfer heat from the heat storage to the load tank is boosted. As a result, configurations with small heat exchangers (733W/K) run, from April to September, with a heat storage tank in average 3°C hotter with Riello collectors and 2.5°C hotter with Solex ones than when large heat exchangers are used (1466W/K) resulting in a lower solar fraction.

Results of simulations and estimated capital cost of the various configurations show that it might be financially beneficial to invest in a more efficient heat exchanger (1466W/K) rather than increasing the surface of panel by 25% (from 16m<sup>2</sup> to 20m<sup>2</sup>), regardless of the type of collector used, see Fig. 18.

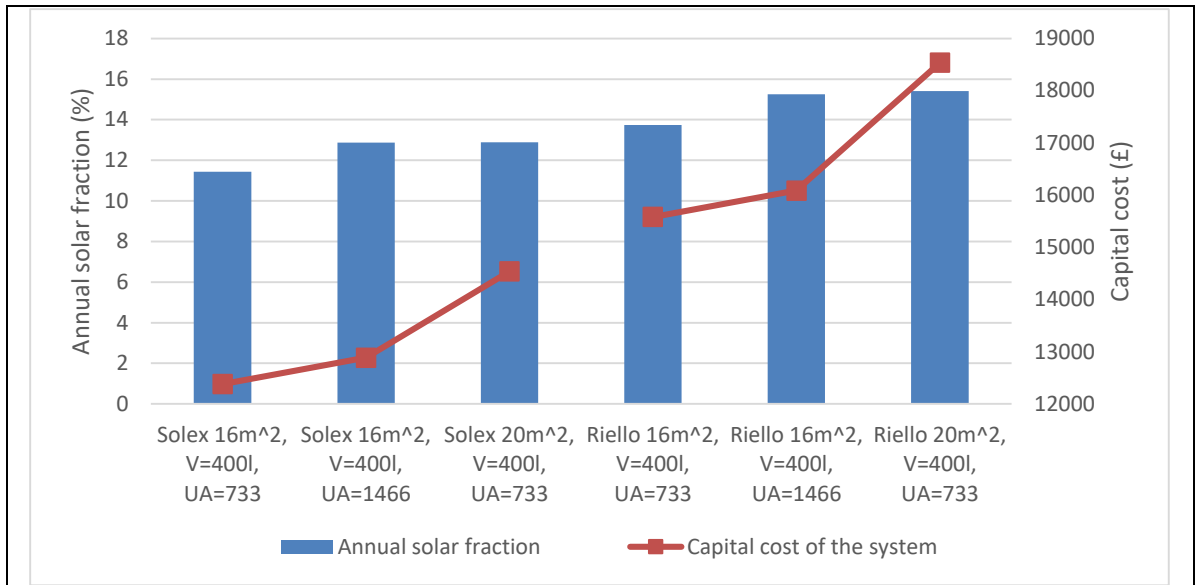


Fig. 18 Impact on the capital cost of the solar system of increasing the characteristics of heat exchangers compared to increasing the surface of collector by 25% in the case of Solex BLUx collectors and Riello CSAO 25R

Fig. 19 shows the impact of both the surface area of collector and UA. A larger surface of panel harvests in principle more energy, but if this energy cannot be transferred at a sufficient rate to the storage tank the working liquid will be hotter thereby reducing the panel efficiency (by 1.87% for Solex and 2.5% for Riello). On the other hand, doubling the capacity of the heat exchanger (from 733W/K to 1466W/K) will increase the rate of heat transfer and decrease the temperature of the working liquid, then efficiency of the collectors is improved (by 4.2% for Solex and 5% for Riello). Riello collectors are less impacted by the change due to their design which allows them to stay more efficient than Solex ones under the same operating conditions.

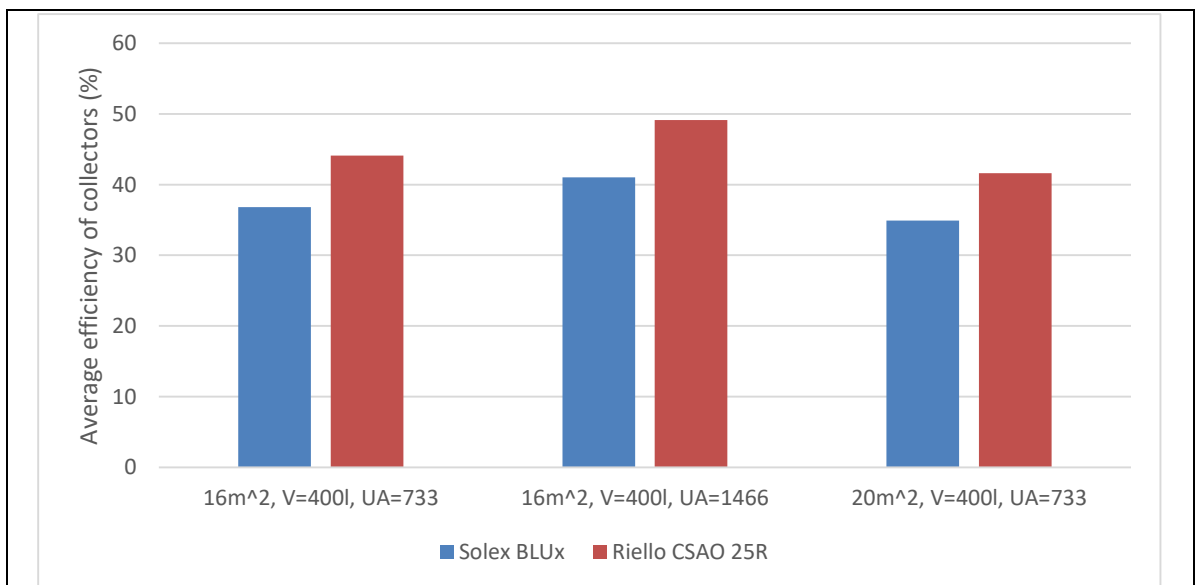


Fig. 19 Average efficiency of the collectors over the month of May for various configurations.

Therefore, there are only advantages to choose heat exchangers with high heat transfer coefficient.

#### 4.1.3 Effect of the solar heat storage tank

According to the results of simulations, the bigger is the volume of the solar heat storage tank and the bigger is the fraction of volume allocated per m<sup>2</sup> of panel, the higher the solar fraction provided by the pre-heating system. These two parameters are, by definition in this study, linked and are set at 20l.m<sup>-2</sup> and 25l.m<sup>-2</sup>. Additionally,

selecting a larger tank has comparatively little impact on the capital cost for sensible improvement of the solar fraction, see Fig. 20.

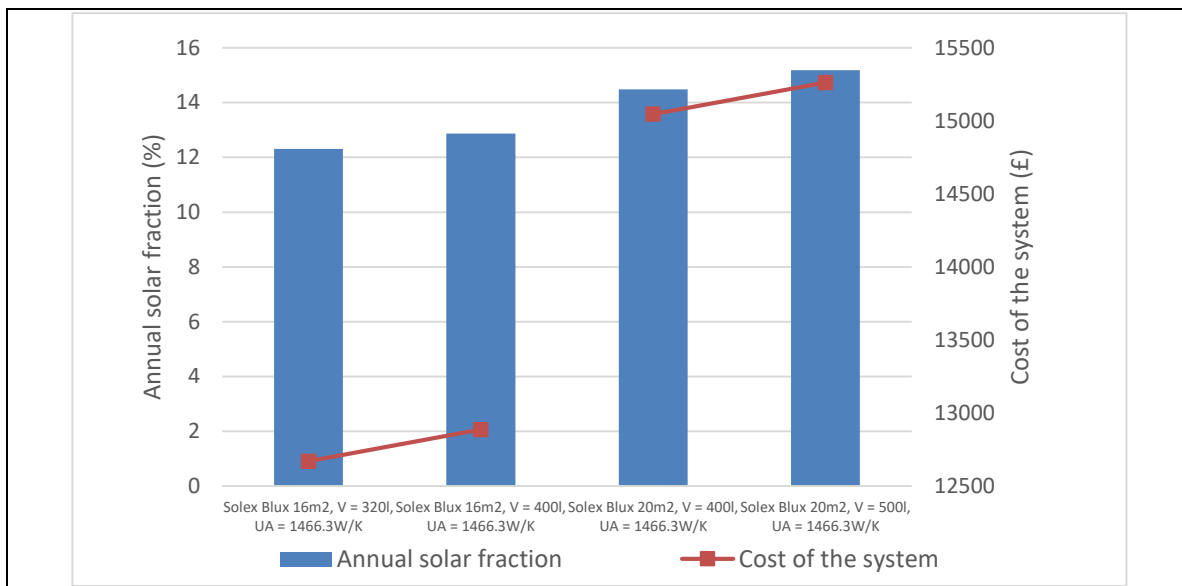


Fig. 20 Influence of the volume of the storage tank on annual solar fraction and capital cost of the system.

For the same configuration of panel and heat exchangers, the average temperature of the heat storage tank (over any month simulated and regardless of the type of panel and heat exchangers) is increased by less than 0.5°C when the allocated volume per m<sup>2</sup> of collector is raised to 25l.m<sup>-2</sup> from 20l.m<sup>-2</sup>. Likewise, the average heat content of the solar storage tank is increased by less than 1kWh. Any appreciable difference resides at the extremes. Table 3 gives the average extremum of heat content for the months of May and January. In summer the type of solar collector appears to have no influence on the maximal heat content which is, for any volume, almost equal to a tank fully heated at 75°C the maximal allowed temperature. Yet it has an influence on the minimal heat content which is in average 2.3 kWh higher when Riello collectors are used. In winter the situation is slightly different and a variation of up to 2 kWh is observed for the maximal heat content, as well as for the minimal one, between configurations using different collectors.

Table 3 Extremum of heat content for various volumes of solar heat storage tanks

Volume of the storage tank (l)	320	400	500
Max heat content May (kWh)	24.21	30.26	37.85
Min heat content May (kWh)	3.329	5.10	5.66
Max heat content January (kWh)	8.44	9.66	13.51
Min heat content January (kWh)	0.20	0.49	0.94

The study of the average effectiveness of solar collectors however shows a decoupling between the effect of the volume allocated per m<sup>2</sup> of panel and the one of the total volume of the tank, see Table 4. For the same volume of storage, decreasing the surface of collector (such as to go from 20l/m<sup>2</sup> to 25l/m<sup>2</sup>) boosts their solar fraction. But for the same fraction of volume per m<sup>2</sup> the bigger the tank the lower the efficiency of collector (verified for any month simulated). If these variations are small (in a range of 4%) they remain noticeable and need some investigations.

Table 4 Simulated efficiency of solar collectors over the month of May 2016, depending on the volume of the storage tank (ST) and the fraction of volume allocated per m<sup>2</sup> of collector.

	320l (20l.m <sup>-2</sup> )	400l (20l.m <sup>-2</sup> )	400l (20l.m <sup>-2</sup> )	500l (20l.m <sup>-2</sup> )
Solex BLUx	40.8	41.0	39.2	39.1
Riello CSAO	48.5	49.1	47.1	46.6

With regard to the first observation an increased volume per m<sup>2</sup> of collector reduces the rate of temperature change in the tank, reducing the temperature of water fed from the tank base to the collector and hence reducing heat losses from the collector (and increasing efficiency).

This conclusion should persist when, for the same fraction of volume per m<sup>2</sup> of panel, the storage tank is increased. Yet, the monthly average efficiency is decreased by 2% when the size is raised from 320l to 400l and from 400l to 500l.

This drop of efficiency remains misunderstood, but is possibly linked to numerical diffusion. The bottom of a bigger tank, which feeds the heat exchanger HX1, will be less affected by the numerical diffusion than a smaller one. Then this volume will stay longer at a low temperature (close to 10°C). Consequently, the heat exchange fluid is maintained at a low temperature at the inlet of solar collectors. Also, the efficiency of the solar collector does not only depend on its own temperature but also on the difference with the ambient air. Therefore, if the average temperature of the panel remains low, its efficiency will be less than if its temperature was closer to the ambient. Thus, a smaller tank might be able to reach faster a more adequate temperature for the functioning of collectors. The numerical diffusion is a purely mathematic issue, however, here, it can compensate for the absence of modelling of mixing effects, hence such observation is expected on real tanks

#### **4.1.4 Effect of solar collectors**

Unsurprisingly, the Riello CSAO 25R collector gives a higher solar fraction than the Solex BLUx in every configuration. For otherwise identical plant, the difference is small in winter (1%), about 4% in spring and autumn, and up to 5.1% in summer.

This higher solar fraction demands more work from the feed pump of collectors P1. The greater amounts of heat collected by the Riello device demand a higher flow-rate (see 3-4) according to equation (10). Fig. 21 shows the difference in pump work for the configuration with 20m<sup>2</sup> of collector, a storage tank of 500l and large heat exchangers (1466W.K<sup>-1</sup>). This increase in pump work will increase the energy bill of the system, but these expenditures are negligible when compared with the savings in gas.

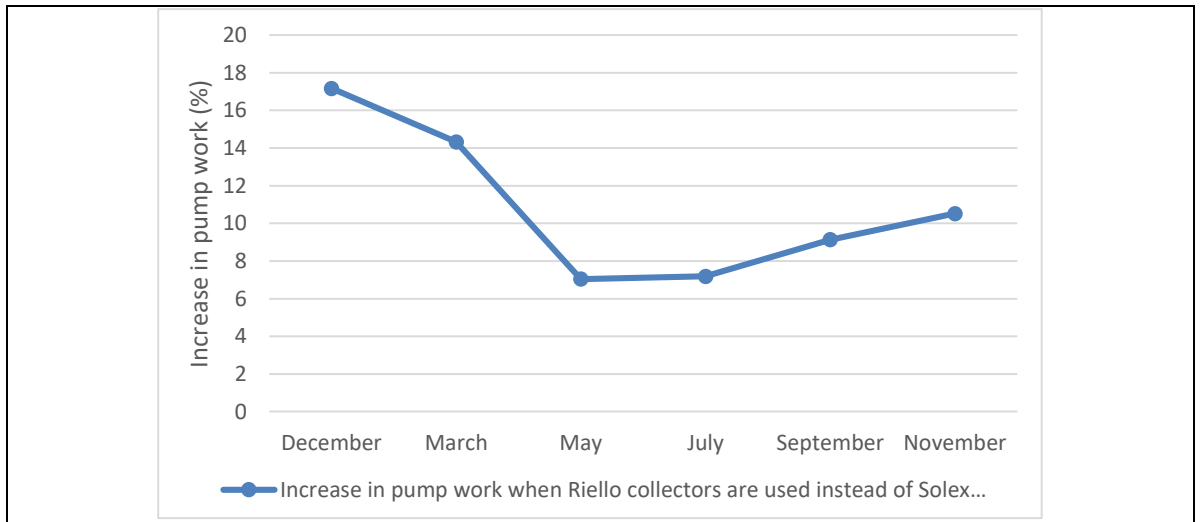


Fig. 21 Increase in work of pump P1 when Riello panels are used instead of Solex ones. Storage tank of 500l and heat exchangers of 1466W/K capacity.

The better performance of the Riello collectors comes at greater capital cost; they are £200 more expensive (£540 instead of £340). Fig. 22 shows the capital cost of same configurations using Riello and Solex panels and the associated solar fraction.

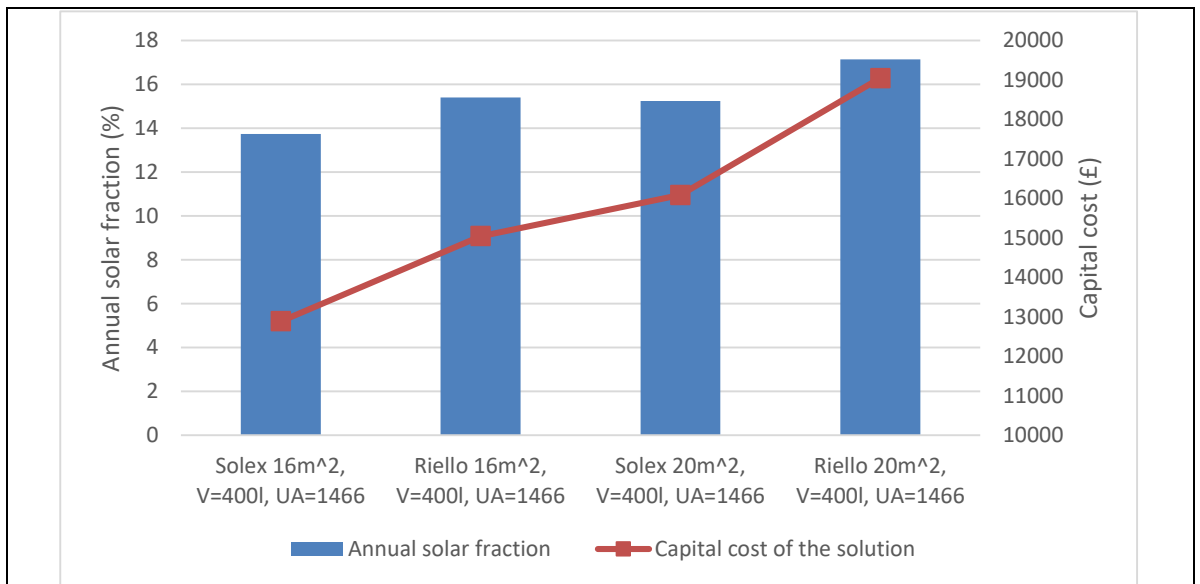


Fig. 22 Example of capital cost increase due to the selection of high efficiency solar collectors (Riello) and its impact on annual solar fraction

## 4.2 COMPLIANCE WITH HEALTH AND SAFETY REQUIREMENTS

Here the focus is made on the temperature of water inside tanks.

### 4.2.1 Load tank

The UK *Health and Safety Executive* require the storage of water above 60°C and its delivery to appliances above 50°C. Not respecting these rules may expose users to hazardous contamination. At the same time, the *Water Regulations Advisory Scheme* (WRAS) recommends that the bottom of the storage has to be heated above 60°C during at least one hour to eradicate the risk of legionella outbreak.

#### ➤ Heating time

The evolution of temperature inside of the two load tanks is prescribed by the daily consumption pattern. However, from one day to another and depending on the quantity of heat available in the heat storage vessel the time for fully heating their content varies.

The more energy in the heat storage tank, the longer the process of heat up of the load tank as the two gas boilers are triggered only when the temperature difference between the top of the storage tank and the bottom of the load tank becomes  $<20^{\circ}\text{C}$ . Also contrary to the gas boilers, the solar storage tank cannot provide a constant heat flow. Then, as seen on Fig. 23, a peak of heat transfer (of maximum 51kW) is provided when the energy starts to be drawn off but rapidly drops. Thus, the pre-heating process cannot be as fast as the boilers.

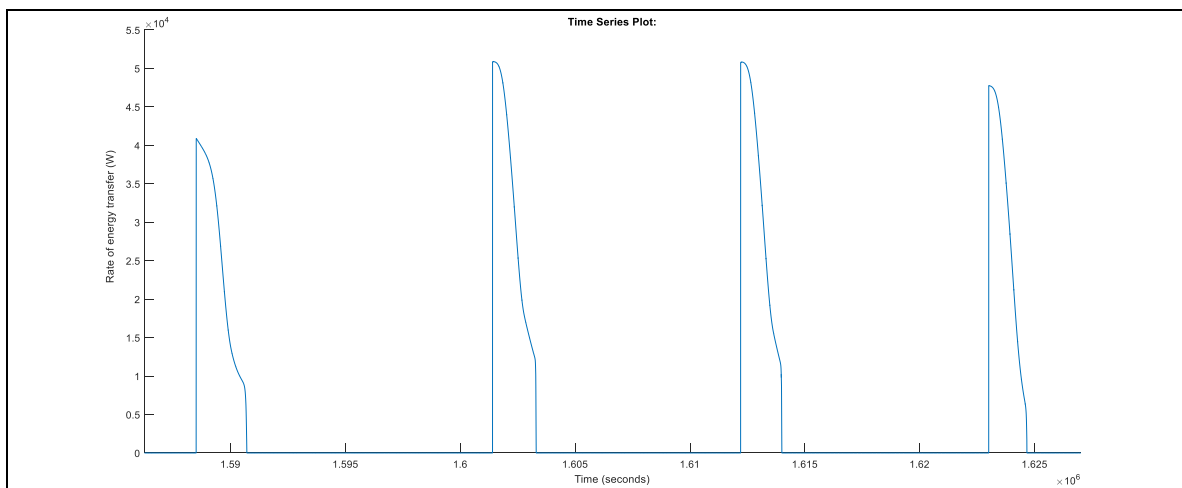


Fig. 23 Example of rate of energy transfer from the heat storage tank to the load tank during the month of May,  $20\text{m}^2$  of Riello collectors, storage volume of 500l and heat exchangers at  $1466\text{W/K}$ .

The time taken by the pre-heating process is difficult to estimate as it depends simultaneously on the volume and temperature of water to “pre-heat” in the load tank and on the quantity of energy available in the heat storage. Globally the heating time ranges from 23min (i.e. time required by gas boilers only) to 38min (for  $20\text{m}^2$  of Riello collectors, storage of 500l and large heat exchangers in May), the process can then be extended by 15min (or by 65%). An example of the difference between heating time for the configuration cited previously in a case of low and high energy content in the storage tank is given in Fig. 24.

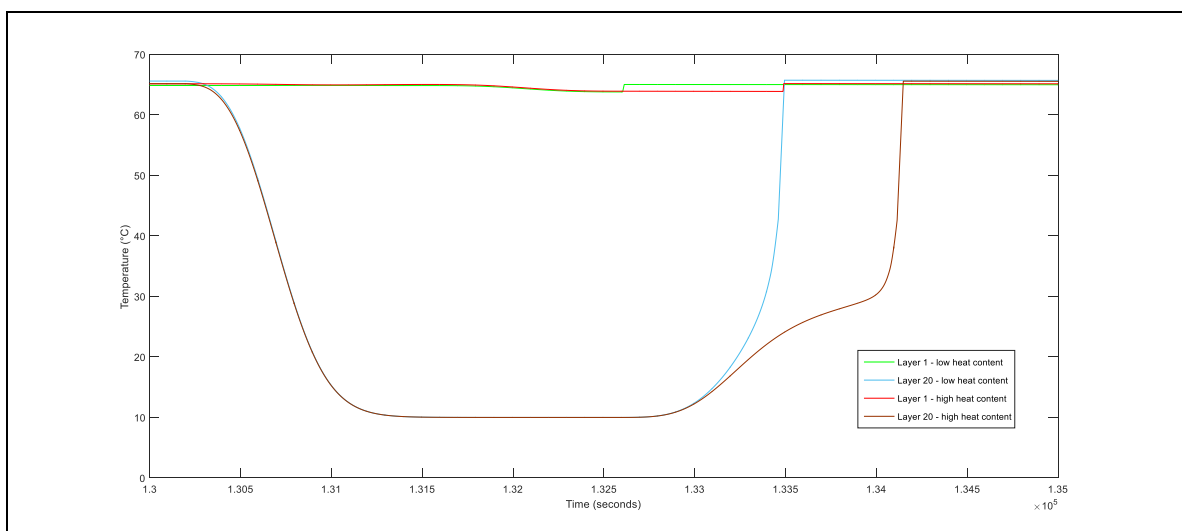


Fig. 24 Temperature development of the top and bottom layers of the load tank during heating process in two cases: low and high heat content in the heat storage tank.  $20\text{m}^2$  of Riello collectors, storage volume of 500l and heat exchangers at  $1466\text{W/K}$ . Layer 1 standing for the top of the tank and layer 20 for its bottom.

With the pattern of consumption used here, the system returns to a fully heated situation before the next peak of consumption. However, if there was less time between peaks, the system might well fail to provide hot water at a legal temperature.

### ➤ Compliance with health and safety rules

The system is, as seen previously, able to return to a fully heated state before the next peak of consumption. The delivery temperature is therefore independent of the configuration of the solar system and the following analysis will be relevant for any of them. A profile of temperature obtained for a day of May with 20m<sup>2</sup> of Riello collectors, storage volume of 500l and heat exchangers at 1466W/K (configuration providing the longest heating times), is plotted in Fig. 25 for illustration.

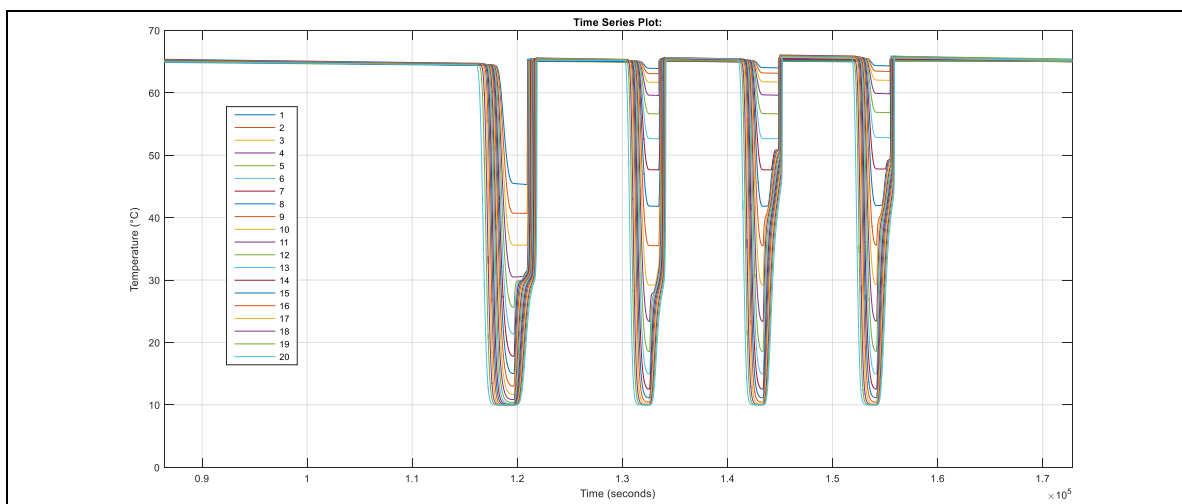


Fig. 25 Temperature of the layers of the one load tank during a day of May, layer 1 being the top of the tank and layer 20 its bottom. 20m<sup>2</sup> of Riello collectors, storage volume of 500l and heat exchangers at 1466W/K

Firstly, Fig. 25 shows water to be provided at a temperature well above the required 50°C during the last three peaks of the day. However, a drop to 45.6°C is observed during the first peak. This temperature is just above the range of multiplication of *Legionella* (20-45°C) and result from the mixing (here diffusion) of water originally at 65°C and water from the feed at 10°C (temperature at which the bacteria is dormant and cannot multiply). Furthermore, this state is temporary and water is rapidly heated to get back to the safe zone. Thus this drop should not be unsafe (but in practice auxiliary heating would be required, at cost). This numerical simulation does need comparison against experiment to ensure that such low temperatures are possible.

Concerning the storage temperature, HSE rules are respected. The tank is fully heated at 65°C during more than one hour between two peaks of consumption, and the temperature stays above 60°C in every layer during the night.

#### 4.2.2 Solar heat storage tank

The solar heat storage tank is biologically isolated from both the solar collector circuit and the two load tanks by intermediate heat exchangers. If HSE rules on storage temperature might be overlooked here, it is still necessary to quantify the potential risks and determine the possible need for additional disinfection means.

#### ➤ Temperature inside of the tank

Contrarily to the load tank, the development of temperature profile inside the heat storage tank changes from one day to another. The variation mainly depends on the initial gradient of temperature at the beginning of the day and on the environmental conditions (which are largely subject to seasonal changes). According to simulations, the highest and lowest peak temperature over any months are obtained respectively with the following configurations (irrespective of the type of collector):

- 20m<sup>2</sup> of collector, 400l of storage, heat exchangers 1466W/K
- 20m<sup>2</sup> of collector, 500l of storage, heat exchangers 1466W/K

The analysis will focus on these two schemes using both Solex and Riello collectors. In winter, the temperature cycles between the range where *Legionella* can grow (20-45°C) and the range where it is dormant (below 20°C), see Fig. 26. Also, the content of the tank never reaches the 60°C threshold for disinfection. Knowing if this behaviour offers adequate conditions for the multiplication of the bacteria goes beyond the range of this project. However, HSE rules are not respected and the safe conclusion to make is that the functioning of the solar system might not be safe during this period, unless an effective biocide is available.

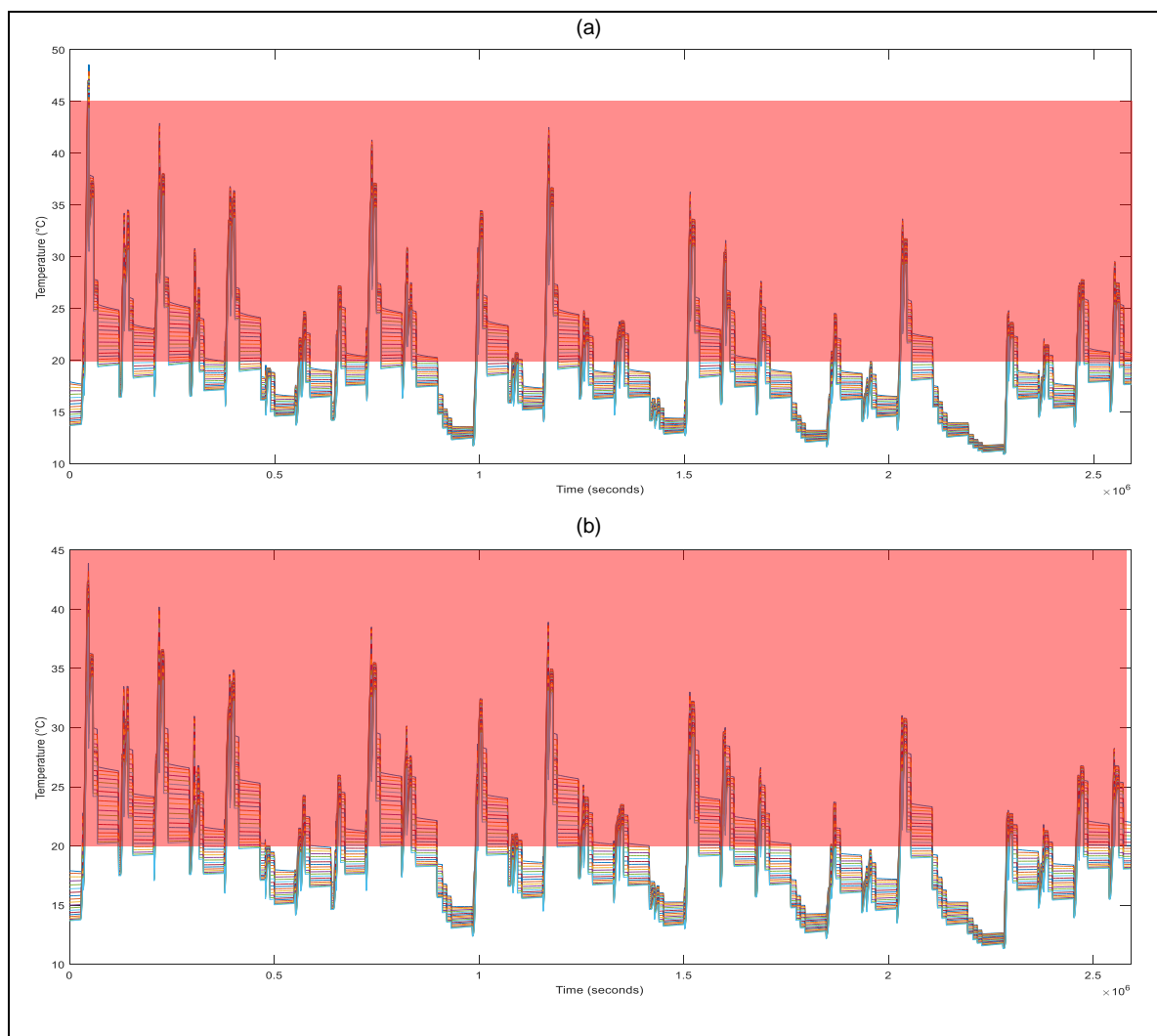


Fig. 26 Simulated temperature profile in the heat storage tank during the month of November when 20m<sup>2</sup> of Solex collectors, large heat exchangers (1466W/K) and a storage volume of (a) 400l, (b) 500l

In mid-seasons (spring and autumn), operating conditions allow water inside of the storage tank to reach higher temperatures than in winter. However, temperatures are pushed up right in the range of *Legionella* growth, as shown on Fig. 27, and barely manage to reach the disinfection threshold of 60°C during one hour. Conditions favour an outbreak as the temperature stays most of the time in the range of growth of *Legionella*, and likely of other bacteria and viruses.

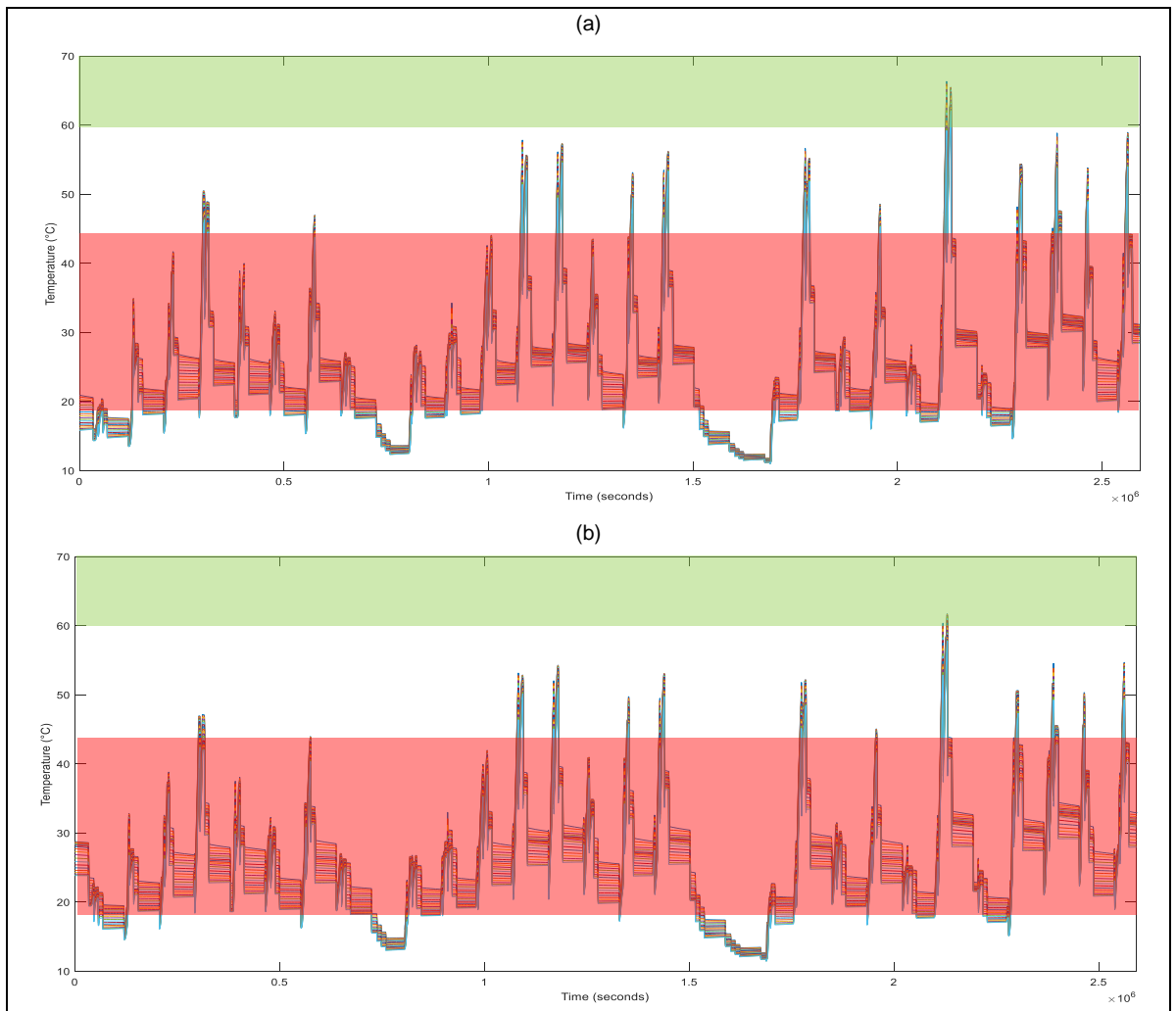


Fig. 27 Simulated temperature profile in the heat storage tank during the month of March when 20m<sup>2</sup> of Solex collectors, large heat exchangers (1466W/K) and a storage volume of (a) 400l, (b) 500l

In summer, operating conditions of solar collectors can allow the heat storage tank to reach the state of maximum allowed 75°C and this during more than one hour per day, even though at this temperature satisfactory disinfection can be achieved in smaller amount of time. The WRAS recommendation can then be met. Fig. 28 (a) and (b) yet highlight two facts, first this full heating state at disinfection temperature is not achieved every day due to the variation in solar intensity. Secondly, water stays in the range of *Legionella* growth most of the time. Beyond the *Legionella* issue, many other organisms grow at these temperatures. Therefore, even if the situation in summer is more acceptable than in winter or mid-season, the solar system is unlikely to guarantee a safe operation.

Riello collectors are able to raise the temperature of the storage tank during all seasons compared to Solex ones. The difference is not much superior to 5°C in general, thus if acceptable conditions can be obtained during summer, the other months will remain problematic. There is definitely a need for both ensuring that the circuit is sealed properly to avoid contamination and guaranteeing that the tank is properly disinfected.

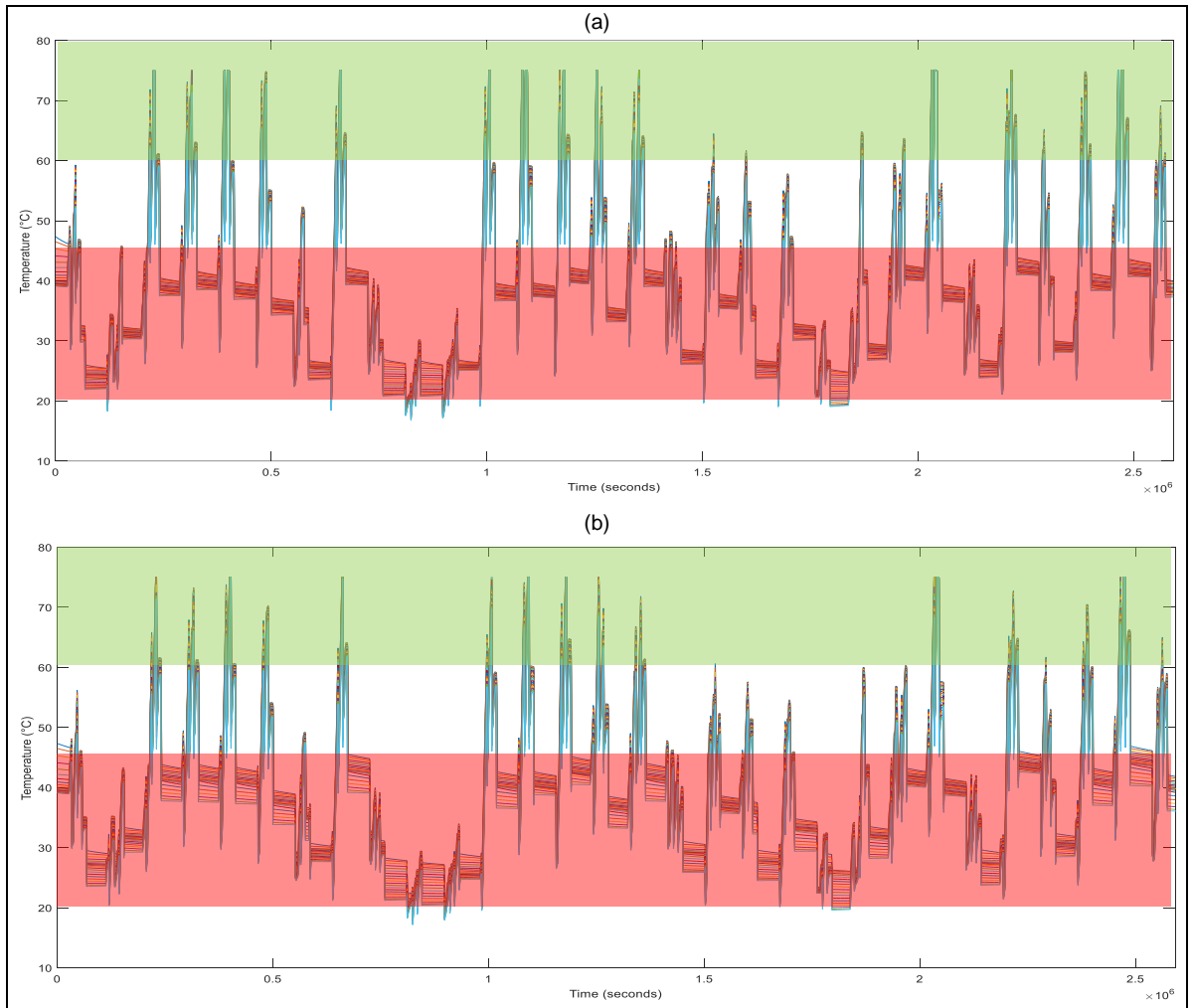


Fig. 28 Simulated temperature profile in the heat storage tank during the month of May when 20m<sup>2</sup> of Solex collectors, large heat exchangers (1466W/K) and a storage volume of (a) 400l, (b) 500l

### ➤ **Solutions for ensuring safety**

Despite the lack of compliance with the safety regulations, technical solutions can be found to ensure that no risk of contamination will emerge.

The first option is to use double-wall heat exchangers to mitigate risk of leaks inside of the heat exchanger. Double wall heat exchangers must be larger than single wall ones for the same capacity of heat transfer and are also more expensive. This solution is prescribed by the *US department of energy* for solar heating installations [58] and seems to be a standard.

Germs and bacteria can be present in the initial water, at the origin on the surface of the components (pipes, tank, heat exchangers) or can be brought during the refill of the tank (if needed). These organisms will not be able to contaminate the load tank but may grow under the favourable conditions of temperature offered. The main risk is a deterioration (creation of a biofilm) or even a clogging of the system leading to additional expenditure for reparation. To prevent any risk, one might treat water of the heat storage tank with a large, but appropriate, quantity of chemical disinfectant (chlorination or super-chlorination). The sealing also makes possible the use of powerful, but not recommended for daily consumption, chemicals such as Bromine or Iodine.

Water could also be replaced by a non-aqueous working fluid such as silicon oil. Though the cost per litre (compared to water) and the regular change of the working fluid should increase the operational expenditures.

### 4.3 FINANCIAL ASSESSMENT

The financial analysis of the various solutions is made on the scenarios identified in Table 2, using rectangular integration of six simulated months.

Using the three parameters identified in part 3-9 (i.e. gas cost, CCL and CCA rates), four scenarios are established for the financial assessment of solutions:

1. DECC central scenario and no discount on CCL
2. DECC high scenario and no discount on CCL
3. DECC central scenario and discount on CCL
4. DECC high scenario and discount on CCL

Since it was found to be an important parameter, the impact of the loan is also introduced in the analysis and three schemes are considered:

- Amortisation over the 25 year-lifespan of the system with interest rate at 6%
- Amortisation over 7 years during which RHI is available, with interest rate at 3.3%
- No amortisation, payment of the capital the year of installation (no loan)

Savings are calculated relative to the estimated operational cost of the current installation which gas consumption is estimated at 51975kWh per year. Results are given in Fig. 29 (a), (b) and (c).

Graphs on Fig. 29 (a) shows that no savings are expected to be made in any scenario when the cost of the system is amortised at a rate of 6% over the 25-year long estimated lifespan of the system. Huge losses, almost equivalent to the price of purchase of the solar pre-heating system (scenario 1), are likely to be suffered.

Diminishing the length and rate of amortisation to 7 years at 3.3% has a positive financial impact, see Fig. 29 (b), losses are reduced by more than 50% in the four scenarios compared to the amortisation over 25 years at 6%. In this case losses are still important for scenario 1,2 and 3 (between £12000 and £2000), however three configurations of the pre-heating system are likely to be marginally profitable when gas cost follows the “high” projection of the DECC and Baddock Hall gets a *Climate Change Agreement* (implying a discount of up to 78% on the CCL tax), i.e. in scenario 4. Details on these systems, their payback and expected savings are given in Table 5. The payback times obtained are extremely long, 23 or 24 years, and make the systems profitable only during the last two years of exploitation, where the likelihood of having a failure of component generally increases.

Table 5 Payback time and expected savings of the three solutions reaching economic viability in the case of a funding with an amortisation over 7 years at 3.3% and scenario 4.

Configuration	Payback time (years)	Savings after 25 years (£)
Solex BLUx 16m <sup>2</sup> , V=400l, UA=1433W/K	23	860
Riello CSAO 16m <sup>2</sup> , V=400l, UA=1433W/K	24	399
Solex BLUx 16m <sup>2</sup> , V=320l, UA=1433W/K	23	382

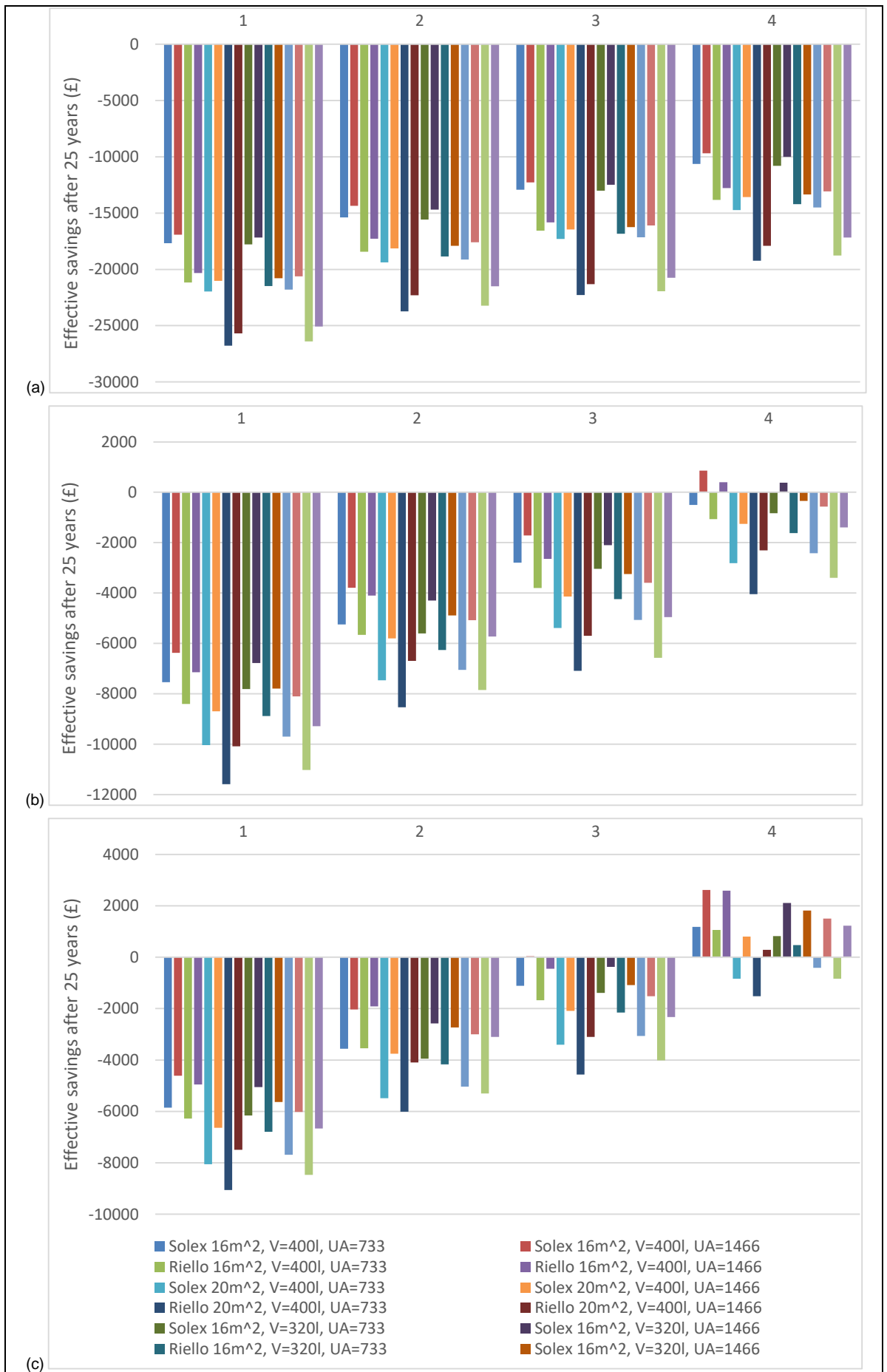


Fig. 29 Expected savings of various configurations of solar pre-heating relatively to the current installation of Baddock Hall. Different types of funding are considered (a) amortisation over 25 years at a rate of 6%, (b) amortisation over 7 years at a rate of 3.3% and (c) payment of the capital at the installation (no loan).

For comparison purpose, a case in which the capital would be paid directly at the installation (equivalent to a loan at 0% rate when inflation is neglected) is considered and plotted in Fig.29 (c). Comparatively to the funding discussed, 7 years at 3.3%, losses are reduced by 20% in scenarios 1,2 and 3 but still remain important (between £9000 and £1000).

In these conditions of funding it appears that the configuration using 16m<sup>2</sup> of Solex BLUx collectors with 400l of solar heat storage and large heat exchangers (UA=1433W/K) reaches the profitability threshold by a short margin of £38 in 24 years in scenario 3. Obviously in reality this balance is unlikely to be reached as over 25 years some reasons (failure, natural disaster...) will probably lead to some unexpected expenditures and put the investment in a situation of deficit.

More interestingly, this way of funding shows that most of the configurations will become profitable in the 4<sup>th</sup> scenario. Table 6 gives the figures for the 6 more financially interesting configurations, the RHI contribution is the total payback granted by the UK government over the 7 first year of exploitation of the solar system.

Table 6 Payback time and expected savings of the six best solution in the case of scenario 3 with payment of the capital at the installation of the system.

Configuration	Payback time (years)	Savings after 25 years (£)	RHI contribution (£)
Solex BLUx 16m <sup>2</sup> , V=400l, UA=1433W/K	19	2616	8988
Riello CSAO 16m <sup>2</sup> , V=400l, UA=1433W/K	20	2591	10591
Solex BLUx 16m <sup>2</sup> , V=320l, UA=1433W/K	20	2108	8595
Riello CSAO 16m <sup>2</sup> , V=320l, UA=1433W/K	21	1817	10087
Solex BLUx 20m <sup>2</sup> , V=500l, UA=1433W/K	22	1507	10552
Riello CSAO 20m <sup>2</sup> , V=500l, UA=1433W/K	23	1229	12458

The payback time is reduced by 4 years compared to a funding with a loan over 7 years at 3.3% for the configuration Solex BLUx 16m<sup>2</sup>, V=400l and large heat exchangers. Still payback times remain long and the breaking point between savings and losses is only reached at the estimated end of life of the system.

Moreover, the total cash flow of money coming from the state through the RHI is significant and can account for more than half of the capital cost of the solar pre-heating system. No configuration of system presented in Table 6 would be profitable without the RHI, the viability of the solar system is then purely artificial.

Table 6 also highlights that, despite a longer payback time, configurations embedding Riello collectors are able to reach almost the same amount of savings than configurations with Solex collectors. This can be explained by the fact that the higher capital cost per m<sup>2</sup> of collector is compensated by the higher efficiency. In the case were the price of high efficiency collectors such as Riello CSAO 25R dropped to the level of standard collectors (such as Solex BLUx), the financial

interest would be increased with expected savings of up to £6298 in the best case (see Fig. 30).

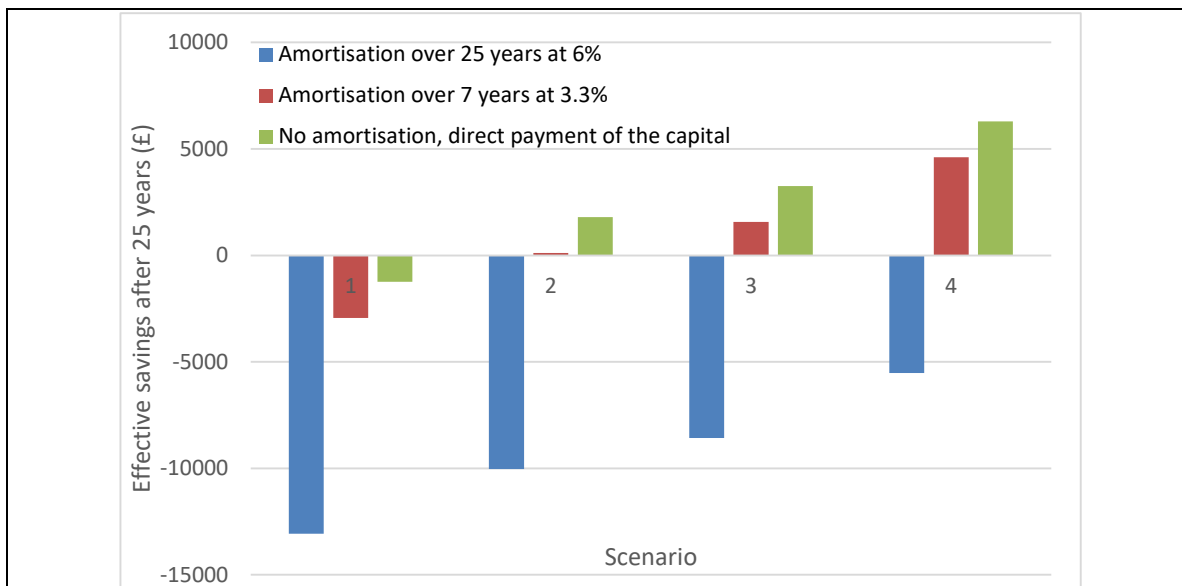


Fig. 30 Savings in various scenarios of gas cost and funding if the price of Riello CSAO 25R collectors was the same than Solex BLUX collectors. Configuration with 16m<sup>2</sup> of collector, storage tank of 400l and heat exchanger of transfer coefficient UA = 1433W/K.

Then the solar pre-heating system for Baddock Hall is only likely to be profitable in a well-defined scenario where:

- The *Sustainability Service* of the University of Bristol manages to get a *Climate Change Agreement* to benefit from a significant discount on the *Climate Change Levy*
- The cost of gas follows the high projections of the DECC
- It is possible to fund the project without a loan, or with a loan at 0% interest
- The *Renewable Heat Incentives* are maintained

Otherwise the additional operational expenditures linked to the maintenance of the solar system and the interests of the loan will completely absorb the savings made. The narrow path which leads to savings being highly hypothetical the safest option, financially speaking, is to keep the actual gas heating system of Baddock Hall unmodified. The study has certainly overestimated the annual fraction by applying the same pattern of consumption every month, even in summer where Baddock Hall is allegedly less crowded.

Nevertheless, a favourable development in the price of the collector and a severe increase in gas cost might lead one to reconsider the project of adding solar pre-heating to the gas unit.

#### 4.4 RECOMMENDATIONS FOR FURTHER WORK

The study has provided interesting results about the use of solar pre-heating for gas heating system. The numerous assumptions are likely to overestimate the solar fraction and the overall efficiency of the system. Here are proposed some ways to improve the reliability of further studies.

- Definition of a better pattern of consumption

The demand defined by Knight, N. gave coherent results in the frame of the electric installation of Baddock Hall. Here, it predicted a gas consumption lower than the range expected in regard to measurements on site. Furthermore, the pattern was repeated every day of the week for the six months simulated. Actually, the occupancy of halls decreases during week-ends and holidays, the volume of hot

water used during these periods should drop. Knight, N. modelled this variation by decreasing arbitrarily the gas consumption. No relevant quantitative information relative to a modification of the consumption were provided for the gas unit and therefore it was not judged relevant to proceed to such a modification of the outputs of simulation.

Defining properly a demand pattern should improve the reliability of these feasibility studies. The determination of the pattern must be able to decouple the effects of central heating, secondary flow and water for consumption. Making appropriate measurements of flow-rates and analysing the resulting dataset should result in the definition of a pattern for Baddock Hall.

Monte-Carlo simulations might be used to define a consumption profile for the bathrooms of the block. This theory [24] aims to generate a database containing the time, the flow-rate and the schedule of use of appliances (sinks, basin, showers) and to create a probability graph of use for each of them. The consumption pattern of a block would then be defined by the superposition of the demand of each appliance. This method gives a high degree of flexibility and repeatability as profiles will not be exactly the same from one day to another, but is also time consuming and requires important means. Yet results could be reused for the study of other accommodations.

➤ Investigation on the pipework and the secondary flow

The total absence of information on the pipework and the secondary flow has forced to neglect them in the study. The discrepancies between gas consumption obtained with the model and the measurements made on site are certainly due to this neglecting. The age of the building probably implies a poor insulation of pipes and important heat losses in the pipework: in the case of the electric heating system return temperatures of the secondary flow were reportedly 10-15°C lower than at the inlet resulting in a cooling of the load tank and thus in an increase in energy consumption. If a proper identification of the return flow is done, it could be worth testing its the heat up with the solar storage tank (by the intermediary of the heat exchanger) before re-injecting it in the tank.

Beyond predicting the gas consumption properly, the pipework is also strongly related to health and safety issue. The HSE edicts some rules relative to the delivery of water in terms of time of residence in the pipe and temperature at the outlet in order to avoid contamination by *Legionella* or other bacteria. As shown previously, the temperature of water drawn off the tank can decrease below 50°C in case of large consumption when HSE recommends a minimum of 50°C at the outlet of appliances. The distribution system is therefore likely not to comply with essential safety rules in some cases. More investigation on the pipework could then be interesting.

Also, instead of trying to reduce the gas consumption by adding a solar pre-heating system, the solution consisting in enhancing the insulation of the pipework could be assessed, though the feasibility and the cost have to be discussed.

➤ Assessment of other configurations – Application to other cases

The architecture of the solar pre-heating system defined in this project has several advantages and gave satisfactory levels of efficiency, however one might try to modify it to reduce the capital cost of the system and/or increase the performances. For instance, configurations with only one heat exchanger between collectors and storage tank, or between storage tank and load tank could be imagined. Also, transferring the energy directly from the collectors to the load tank could be a solution. Capital cost can be decreased, but the different issues emerging with modified architectures are probably difficult to solve.

Also, an application to other heating systems using other sources of energy than gas will potentially give interesting results on potential savings. The current high price of electricity (4 to 5 times more expensive than gas per kWh) makes electric system perfect candidates for a refit. The physics embedded in tank heated with electric resistance will yet require a modification of the model. The current electric unit of Baddock Hall is old and obsolete, applying pre-heating could give positive results and even profitability in the least positive scenario for renewables (i.e. no CCL discount and “central” path for electricity cost).

➤ The need for *Demand Side Management* strategies

*Demand Side Management* (DSM) consists in enticing people to change their way of using energy. Extensive literature is available on DSM strategies applied to electric heating, but little to nothing is about managing solar energy.

The efficiency of the solar system depends on both the quantity of energy harvested and stored in the storage tank and the quality of the heat stored (i.e. the temperature of water). High grade heat will pre-heat faster and to higher temperature than low grade one. Therefore, it could be interesting to investigate and determine the moments at which peaks of consumption have to happen to optimise the functioning of the solar system, i.e. when the heat storage tank is fully heated or at least when it reaches its potential maximal heat content of the day. The DSM also has to find ways to sensitize students to use hot water at these appropriate moments. Then, a good DSM strategy can help improving the efficiency of the solar system but also manage to reduce the overall consumption of energy in the residence.

## 5 Conclusion

The model developed in this project gave a coherent simulation of solar assisted gas boiler in the context of a university hall of residence. Despite the lack of some crucial information, the predicted gas consumption remains very broadly in the range given by real measurements. The model is also flexible enough to be modified or reused as such in further studies.

The interest of solar pre-heating for gas boilers has been highlighted, high levels of solar fraction can be reached with a careful selection of the components of the system. Up to 36% of the energy can be provided by the sun during summer months and 18% annually. At the same time, it has also been demonstrated that the solar system will have adequate efficiency over only half of the year. A suitable solar fraction is then available only when the requirement for hot water is at its lowest (hot period). This conclusion is true for solar heating systems in general.

Health and safety requirements can be met in the load tank, but not in the solar heat storage tank. Additional means to control the purity were proposed; the use of chemical disinfectant seems to be the easiest solution. Basic rules like regular maintenance and use of double-wall heat exchangers will ensure the safety of the installation.

The system with highest solar fraction also has the highest capital cost and is not the best system financially. However, the best solution embeds 16m<sup>2</sup> of Solex BLUX panels, a storage volume of 400l and heat exchangers of capacity 1466W.K<sup>-1</sup>. It is worth noting that this solution has large heat exchangers and allocate 25l.m<sup>-2</sup> in the storage tank, two factors which were proved to increase the solar fraction.

The feasibility of investing in such a refit of the current gas heating system of Baddock Hall, is questionable. Savings are only likely to be made in the case where the cost of gas follows the “high” prediction of the DECC and the *Sustainability Service* manages to get a CCA to grant the discount on CCL. Moreover, the capital of the system would have to be paid directly (without loan). Even in these circumstances savings will be limited to the order of £2000 after 25 years with a payback time of 19 years, close to the end of system lifetime. The risk of the investment is then high, particularly if energy consumption has been overestimated.

Solar pre-heating will have to be reconsidered should the cost of solar collectors decrease (and still perform well, e.g. the Riello CSAO 25R). Also, if this solution is not likely to result in savings in the case of a gas fired unit, its fitting to an electric or oil fired unit might become interesting as the cost per kWh of these energy is 2 to 5 times greater than natural gas.

Further analyses of Baddock Hall installations are clearly required to allow complementary work on the subject. Also it would be useful to investigate the pattern of hot water consumption to manage to find an optimal functioning of the solar pre-heating system. These factors will however not make the system be more financially viable, the only mean to end the superiority of gas being a strong increase in its cost per kWh.

## 6 References

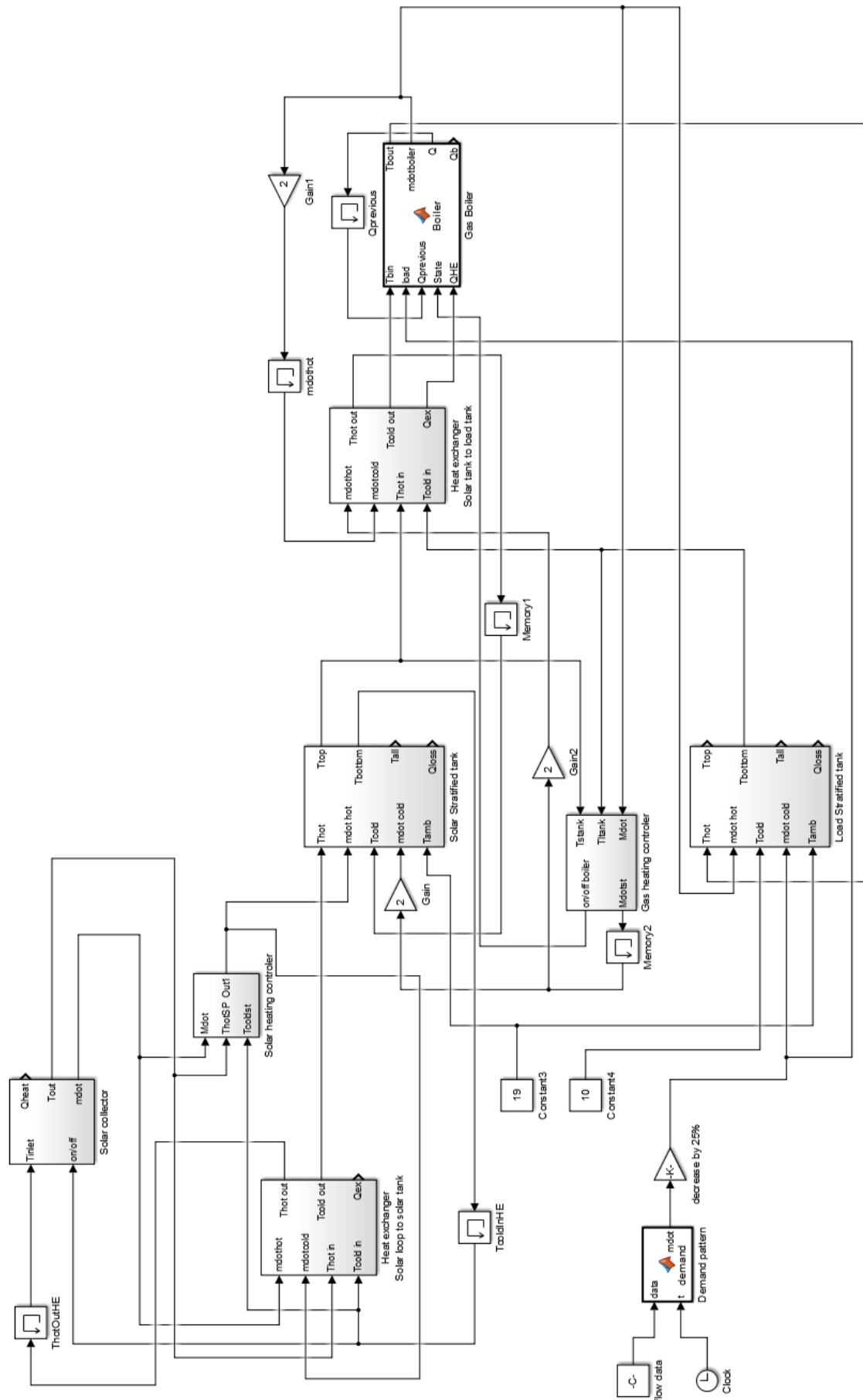
- [1] Department of Energy and Climate Change (2012), *United Kingdom Housing Energy Fact File*, London: Palmer, J. and Cooper, I.
- [2] Hot Water Association (HWA) (2010), *Heating and hot water pathways to 2020*. London: Author.
- [3] UK Government (2016), *Climate Change Levy rates*, [Online]. Available: <https://www.gov.uk/government/publications/rates-and-allowances-climate-change-levy/climate-change-levy-rates>. [Accessed: 10-Sept-2016].
- [4] The Energy Saving Trust (2016), *Renewable Heat Incentive*. [Online]. Available: <http://www.energysavingtrust.org.uk/renewable-heat-incentive>. [Accessed: 10-Sept-2016].
- [5] R. Hastings and M. Wall (2009), *Sustainable Solar Housing*, London: Earthscan.
- [6] Institut für Solartechnik (SPF), Test reports: Collectors, [Online]. Available: <http://www.spf.ch/Collectors.111.0.html?&L=6>. [Accessed: 10-Sept-2016].
- [7] Lavan, Z. and Thompson, J. (1976) 'Experimental study of thermally stratified hot water storage tanks', *Solar Energy*, vol. 19, pp. 519-524.
- [8] Han, Y.M. *et al* (2008) 'Thermal stratification within the water tank', *Renewable and Sustainable Energy Reviews*, vol. 13, pp. 1014-1026.
- [9] Campos Celador, A. *et al* (2011) 'Implications of the modelling of stratified hot water storage tanks in the simulation of CHP plants', *Energy Conversion and Management*, vol. 52, pp. 3018-3028
- [10] Nelson, J.E.B. *et al* (1997) 'Parametric studies on thermally stratified chilled water storage systems', *Applied Thermal Engineering*, vol. 19, pp. 89-115.
- [11] Alizadeh, S. (1999) 'An experimental and numerical study of thermal stratification in a horizontal cylindrical solar storage tank', *Solar Energy*, vol. 66, no. 6, pp. 409-421.
- [12] Chartered Institution of Building Services Engineers (2014) *Public health and plumbing engineering (CIBSE Guide G)*, 3<sup>rd</sup> edition, London: Authors.
- [13] Ferguson-Brown Sustainable Engineering Ltd (2016) *University of Bristol Student Halls of Residence Badock Hall Blocks 2 - 3 and Hiatt Baker Hall Blocks C-D – Hot Water Energy Consumption Analysis*, revision 01, Bristol: Authors.
- [14] Buderus, Bosch Technology Ltd (2011) *Solar thermal technology for large-scale hot water and central heating backup*, [Online]. Available: <http://www.buderus.co.uk/files/201107211309510.BBT2247%20Solar%20Planning%20Guide.pdf>. [Accessed: 10-Sept-2016]
- [15] Kalogirou, S. A. (2004) 'Solar thermal collectors and applications', *Progress in Energy and Combustion Science*, vol. 30, pp. 231-295.
- [16] Institut für Solartechnik SPF (2016) *Solar collector factsheet: Riello BE CSAO 25R*, [Online]. Available: <http://www.spf.ch/fileadmin/daten/reportInterface/kollektoren/factsheets/scf1696fr.pdf>. [Accessed: 10-Sept-2016].
- [17] Institut für Solartechnik SPF (2014) *Solar collector factsheet: Solex BLUx*, [Online]. Available: <http://www.spf.ch/fileadmin/daten/reportInterface/kollektoren/factsheets/scf1637fr.pdf>. [Accessed: 10-Sept-2016].
- [18] Debrunner Acifer (shop-da.dkch.ch) *Capteur solaire CSAO 25R*, [Online]. Available: <http://shop-da.dkch.ch/product.cfm?dim=905.524&sprache=f&CFID=10386983&CFTOKEN=8e30e2eb9bbf591b-1A14B4BE-E1C7-2C70-3279773FDE4A2456>. [Accessed: 10-Sept-2016].
- [19] Sunerg Solar s.r.l (2011) *Solar Thermal Catalogue*, [Online]. Available: <http://www.solarzone.ro/manuale-tehnice/Catalog-Sunerg-Panouri-Solare-Termice-2011.pdf>. [Accessed: 10-Sept-2016].
- [20] Department for Environment Food and Rural Affairs (DEFRA), (2008) *Measurement of domestic hot water consumption in dwellings*, London: Authors.

- [21] Papakostas, K.T. *et al* (1995) 'Residential hot water use patterns in Greece', *Solar Energy*, vol. 54, no. 6, pp. 369-374.
- [22] Meyer, J.P. and Tshimankinda, M. (1997) 'Domestic hot water consumption in South African Houses for developed and developing communities', *International Journal of Energy Research*, vol. 21, pp. 667-673.
- [23] Wise, A.F.E. And Swaffield, J.A. (2002) *Water, sanitary & waste services for buildings*, 5<sup>th</sup> edition, Oxford: Butterworth-Heinemann.
- [24] Mui, K.W. and Wong, L.T. (2011) 'A comparison between the fixture unit approach and Monte-Carlo simulation for designing water distribution systems in high-rise buildings', *Water SA*, vol. 37, no. 1, January, pp. 109-114.
- [25] Health and Safety Executive (HSE) (2014) *Legionnaires' disease, Part 2: The control of Legionella in hot and cold water systems*, [Online]. Available: <http://www.hse.gov.uk/pubns/priced/hsg274part2.pdf>. [Accessed: 10-Sept-2016].
- [26] Health and Safety Executive (HSE) (2012) *Managing the risks from hot water and surfaces in health and social care*. [Online] Available: <http://www.hse.gov.uk/pubns/hsis6.pdf>. [Accessed: 10-Sept-2016].
- [27] Makin, T. (2013) 'Storage of preheated domestic hot water and possible growth of Legionella bacteria', London: Water Regulations Advisory Schemes, [Online]. Available: [https://www.wras.co.uk/downloads/public\\_area/publications/general/preheated\\_water\\_Nov\\_2014.pdf](https://www.wras.co.uk/downloads/public_area/publications/general/preheated_water_Nov_2014.pdf). [Accessed: 10-Sept-2016].
- [28] Culp, G.L. and Culp, R.L. (1974) *New concepts in water purification*, New York: Van Nostrand Environmental Engineering Series.
- [29] Binnie, C. and Kimber, M. (2009) *Basic Water Treatments*, 4<sup>th</sup> Edition, London: Thomas Telford Limited.
- [30] Pandit, A.B. and Kumar, J.K. (2012) *Drinking water disinfection techniques*, New York: Taylor & Francis Group.
- [31] Kim, B.R. *et al* (2002) 'Literature review-efficacy of various disinfectants against *Legionella* in water systems', *Water Research*, vol. 36, no. 18, pp. 4433-4444
- [32] Anderson, A.C. *et al* (1982) 'A brief review of the current status of alternatives to chlorine disinfection of water', *American Journal of Public Health*, vol. 72, no. 11, pp. 1290-1292.
- [33] Magde, B.A. and Jensen, J.N. (2002) 'Disinfection of wastewater using a 20kHz ultrasound unit', *Water Environment Research*, vol. 74, no. 2; March-April, pp. 159-169.
- [34] Hua, I. and Thompson, J.E. (2000) 'Inactivation of *Escherichia coli* by sonication at discrete ultrasonic frequencies', *Water Research*, vol. 34, no. 15, pp. 3888-3893.
- [35] U.S Department of Energy (2016) *Saving Project: Insulate your water heater tank*, [Online]. Available: <http://energy.gov/energysaver/projects/savings-project-insulate-your-water-heater-tank>. [Accessed: 10-Sept-2016].
- [36] Jarfelt, U. and Ramnäs O. (2006) 'Thermal conductivity of polyurethane foam – best performance', *Skeption 6 a: Heat distribution – pipe properties*, 10<sup>th</sup> International Symposium on District Heating and Cooling, Goteborg, pp. 3-5.
- [37] Chartered Institution of Building Services Engineers (2007) *Reference data (CIBSE Guide C)*, London: Authors.
- [38] Northern Lights Solar Solutions *Solar Plate Heat Exchanger*, [Online]. Available: <http://www.solartubs.com/solar-plate-heat-exchanger.html>. [Accessed: 10-Sept-2016].
- [39] Institut für Solartechnik (SPF), Test reports: Explanations, [Online]. Available: <http://www.spf.ch/index.php?id=203&L=6>. [Accessed: 10-Sept-2016].
- [40] Duffie, J. A. and Beckman, W. A. (2013) *Solar Engineering of Thermal Processes*, 4<sup>th</sup> edition, London: Wiley.
- [41] European Solar Thermal Industry Federation (2012) *Quality Assurance in Solar Heating and Cooling Technology: A Guide To The Standard EN12975*. Brussels: Authors.
- [42] Institut für Solartechnik (SPF) [Online]. <http://www.spf.ch>. [Accessed: 10-Sept-2016].
- [43] Nhut, L. M. and Park, Y. C. (2013) 'A study on automatic optimal operation of a pump for solar domestic hot water system', *Solar Energy*, vol. 98, pp. 448-457.

- [44] VDI-Verlag GmbH (1991) *VDI-Warmeatlas: Table 8-3-1 – Properties of mixture Water/Glycol*, Dusseldorf: Authors.
- [45] Hicks, M. weather station website, [Online]. Available: <http://www.martynhicks.uk/weather/data.php>. [Accessed: 10-Sept-2016].
- [46] Versteeg, H. K. and Malalasekera, W.(1995) *An Introduction to Computational Fluid Dynamics – The Finite Volume Method*, Harlow: Longman Group Ltd.
- [47] Taylor, G. (1954) 'The dispersion of matter in turbulent flow through a pipe', *Proceedings of the Royal Society of London A: Mathematical, Physical and Engineering Sciences*, vol. 223, no. 1155, pp. 446-468.
- [48] Knight, N. (2016) *The most acceptable method for heating at 'Baddock' – A University of Bristol Hall of Residence*, Bristol: University of Bristol - Department of Mechanical Engineering
- [49] European Commission – Institute for Energy and Transport (IET), *Interactive maps and animations*, [Online]. Available: <http://re.jrc.ec.europa.eu/pvgis/imaps/index.htm>. [Accessed: 10-Sept-2016].
- [50] Hicks, M. weather station website, *Archive database query functions for Horfield/Filton basic weather data*, [Online]. Available: <http://www.martynhicks.uk/weather/wxsqldold.php>. [Accessed: 10-Sept-2016].
- [51] Alfa-Laval (2012) *Pricelist: Comfort and general industry equipment*
- [52] Grundfos (2016) *Product Catalogue*, [Online]. Available: <http://product-selection.grundfos.com/catalogue.html?cmpid=ps%3Agoogle%3Agpc%3Agpu%3A%2Bgrundfos+%2Bcatalogue>. [Accessed: 10-Sept-2016].
- [53] Energy Saving Trust (2016) *Solar Water Heating*, [Online]. Available: <http://www.energysavingtrust.org.uk/renewable-energy/heat/solar-water-heating>. [Accessed: 10-Sept-2016].
- [54] Wondrausch, G. (2011) 'Solar Thermal – a guides to life expectancy and maintenance', *YouGen* [Online]. Available: <http://www.yougen.co.uk/blog-entry/1765/Solar+Thermal++a+guide+to+life+expectancy+and+maintenance>. [Accessed: 10-Sept-2016].
- [55] Department of Energy and Climate Change (2015) *DECC2015 Fossil Fuels Price Assumptions*, [Online]. Available: [https://www.gov.uk/government/uploads/system/uploads/attachment\\_data/file/477958/2015\\_DECC\\_fossil\\_fuel\\_price\\_assumptions.pdf](https://www.gov.uk/government/uploads/system/uploads/attachment_data/file/477958/2015_DECC_fossil_fuel_price_assumptions.pdf). [Accessed: 10-Sept-2016].
- [56] Deloitte (2013) *Oil and gas taxation in the UK*, London: Authors.
- [57] Boxwell, M. (2016) *Solar Electricity Handbook*, London: Greenstream Publishing
- [58] U.S. Department of Energy (2016) *Heat exchangers for solar water heating*, [Online]. Available: <http://energy.gov/energysaver/heat-exchangers-solar-water-heating-systems>. [Accessed: 10-Sept-2016].

# Appendix

## APPENDIX A SIMULINK MODEL OF THE PROPOSED SOLAR ASSISTED PLANT



## APPENDIX B IMPLEMENTATION OF STRATIFIED TANKS

### ➤ *Matlab code of inside 'Solar stratified tank' block*

```
function [sys,x0,str,ts,simStateCompliance] = Stratification_modified_4_solar
(t,x,u,flag)

N = 20; % Number of nodes

switch flag,

    case 0,
        str = [];
        ts = [0 0];

        sizes = simsizes;% set up a simsizes structure.
        sizes.NumContStates = N+2; % Number of continuous states
        sizes.NumDiscStates = 0;
        sizes.NumOutputs = N+1; % Two numerical outputs
        sizes.NumInputs = 5; % Four numerical inputs
        sizes.DirFeedthrough = 1; % Matrix D is nonempty.
        sizes.NumSampleTimes = 1;
        simStateCompliance = 'DefaultSimState';
        sys = simsizes(sizes);
        x0 = Initial gradient of temperature 22*1 array;

    case 1,
        mdothot = u(1);
        mdotcold = u(2);
        Thot = u(3);
        Tcold = u(4);
        Tamb = u(5);

        sys = process(t,x,mdothot,mdotcold,Thot,Tcold,Tamb,N);

    case 2,
        sys = [];

    case 3,
        sys = zeros(1,N+1);
        for i=1:N
            sys(i) = x(N+2-i);
        end

        sum = 0;
        for i = 2:N+1
            sum = sum + 0.24*0.6*pi*1.8/N*(u(5) - x(i));
        end
        sys(N+1) = sum;

    case 4,
        sys = [];

    case 9,
        sys = [];

    otherwise
        DAStudio.error('Simulink:blockks:unhandledFlag', num2str(flag));

end
end

function dx = process(t,x,mdothot,mdotcold,Thot,Tcold,Tamb,N)

rho = 1000; % kg/m^3
r = 0.3;%0.35;%0.25; %0.33;% m, radius of the cylindrical tank
A = pi*r^2; % m^2
P = 2*pi*r; % m
kf = 0.6; % W/(m.K)
cp = 4186; % J/(kg.K)
U = 0.24; % W/(K.m)
h = 1.8/N;%1.05/N;%1.46/N;%
```

```

dx1 = 0;
dx2 = 0;

if t > 38002
    f=0;
end

if mdothot == 0 && mdotcold == 0
elseif mdothot > 0 && mdotcold == 0
    x(N+2) = Thot;
elseif mdotcold > 0 && mdothot == 0
    x(1) = Tcold;
elseif mdothot > 0 && mdotcold > 0
    x(1) = Tcold;
    x(N+2) = Thot;
end

if mdothot == 0 && mdotcold == 0
    x(1) = x(2);
    x(N+2) = x(N+1);
    d2Tdx2 = cat(1,0,diff(diff(x)),0)/(h^2) ;
    dx1 = U*P/(A*rho*cp)*(Tamb-x) + kf/(rho*cp)*d2Tdx2 ;
else
    if mdotcold > 0
        mdot = mdotcold;
        ic = 2;

        while ic < N+2
            if Tcold > x(ic)
                ic = ic + 1;
            else
                break
            end
        end

        if ic == 2
            x(1) = Tcold;
            x(N+2) = x(N+1);
            dTdx = cat(1,0,diff(x)) /h ;
            d2Tdx2 = cat(1,0,diff(diff(x)),0)/(h^2) ;
            dx1 = -mdot/(rho*A)*dTdx + U*P/(A*rho*cp)*(Tamb-x) +
kf/(rho*cp)*d2Tdx2 ;
        else
            x(1) = x(2);
            x(N+2) = x(N+1);
            y = [Tcold; x(ic:N+2)];
            dTdx = cat(1,0,diff(y)) /h ;
            dTdx = [zeros(ic-1,1); dTdx(2:(N+2-ic+2))];
            d2Tdx2 = cat(1,0,diff(diff(x)),0)/(h^2) ;
            dx1 = -mdot/(rho*A)*dTdx+ U*P/(A*rho*cp)*(Tamb-x) +
kf/(rho*cp)*d2Tdx2;
        end
    end

    if mdothot > 0
        mdot = mdothot;
        ih = N+1;

        while ih > 1
            if Thot < x(ih) || x(ih) > 75
                ih = ih-1;
            else
                break
            end
        end

        if ih == N+1
            x(1) = x(2);
            x(N+2) = Thot;
            dTdx = cat(1,-diff(x),0) /h ;
            d2Tdx2 = cat(1,0,diff(diff(x)),0)/(h^2) ;

```

```

        dx2 = -mdot/(rho*A)*dTdx+ U*P/(A*rho*cp)*(Tamb-x) +
kf/(rho*cp)*d2Tdx2 ;
    else
        x(1) = x(2);
        x(N+2) = x(N+1);
        y = [x(1:ih); Thot];
        dTdx = cat(1,-diff(y),0) /h ;
        dTdx = [dTdx(1:ih); zeros(N+2-ih,1)];
        d2Tdx2 = cat(1,0,diff(diff(x)),0)/(h^2) ;
        dx2 = -mdot/(rho*A)*dTdx+ U*P/(A*rho*cp)*(Tamb-x) +
kf/(rho*cp)*d2Tdx2;
    end
end
end
if t > 33620
    f=0;
end
dx = dx1 + dx2;
end

```

### ➤ **Matlab code of inside 'Load stratified tank' block**

```

function [sys,x0,str,ts,simStateCompliance] = Stratification_modified_3 (t,x,u,flag)

N = 20; % Number of nodes

switch flag,

    case 0,
        str = [];
        ts = [0 0];

        sizes = simsizes;% set up a simsizes structure.
        sizes.NumContStates = N+2; % Number of continuous states
        sizes.NumDiscStates = 0;
        sizes.NumOutputs = N+1; % Two numerical outputs
        sizes.NumInputs = 5; % Four numerical inputs
        sizes.DirFeedthrough = 1; % Matrix D is nonempty.
        sizes.NumSampleTimes = 1;
        simStateCompliance = 'DefaultSimState';
        sys = simsizes(sizes);

        x0 = 64.78*ones(N+2,1);

    case 1,
        mdothot = u(1);
        mdotcold = u(2);
        Thot = u(3);
        Tcold = u(4);
        Tamb = u(5);

        sys = process(t,x,mdothot,mdotcold,Thot,Tcold,Tamb,N);

    case 2,
        sys = [];

    case 3,
        sys = zeros(1,N+1);
        for i=1:N
            sys(i) = x(N+2-i);
        end

        sum = 0;
        for i = 2:N+1
            sum = sum + 0.24*0.2725*2*pi*1.45/N*(u(5) - x(i));
        end
        sys(N+1) = sum;

    case 4,
        sys = [];

    case 9,
        sys = [];

    otherwise
        DAStudio.error('Simulink:blockks:unhandledFlag', num2str(flag));

end
end

```

```

function dx = process(t,x,mdothot,mdotcold,Thot,Tcold,Tamb,N)

rho = 1000; % kg/m^3
r = 0.2725; % m, radius of the cylindrical tank
A = pi*r^2; % m^2
P = 2*pi*r; % m
kf = 0.6; % W/(m.K)
cp = 4186; % J/(kg.K)
U = 0.24; %0.237; % W/(K.m)
h = 1.45/N;

dx1 = 0;
dx2 = 0;

if mdothot == 0 && mdotcold == 0
elseif mdothot > 0 && mdotcold == 0
    x(N+2) = Thot;
elseif mdotcold > 0 && mdothot == 0
    x(1) = Tcold;
elseif mdothot > 0 && mdotcold > 0
    x(1) = Tcold;
    x(N+2) = Thot;
end

if t > 100
    f = 0;
end

if mdothot == 0 && mdotcold == 0
    x(1) = x(2);
    x(N+2) = x(N+1);
    d2Tdx2 = cat(1,0,diff(diff(x)),0)/(h^2) ;
    dx1 = U*P/(A*rho*cp)*(Tamb-x) + kf/(rho*cp)*d2Tdx2 ;
else
    if mdotcold > 0
        x(N+2) = x(N+1);
        mdot = mdotcold;
        dTdx = cat(1,0,diff(x) ) /h ;
        d2Tdx2 = cat(1,0,diff(diff(x)),0)/(h^2) ;
        dx1 = -mdot/(rho*A)*dTdx + U*P/(A*rho*cp)*(Tamb-x) + kf/(rho*cp)*d2Tdx2 ;
    end

    if mdothot > 0
        mdot = mdothot;
        ih = N+1;

        while ih > 1
            if Thot < x(ih) || x(ih) > 65
                ih = ih-1;
            else
                break
            end
        end

        if ih == N+1
            x(1) = x(2);
            x(N+2) = Thot;
            dTdx = cat(1,-diff(x),0) /h ;
            d2Tdx2 = cat(1,0,diff(diff(x)),0)/(h^2) ;
            dx2 = -mdot/(rho*A)*dTdx+ U*P/(A*rho*cp)*(Tamb-x) + kf/(rho*cp)*d2Tdx2 ;
        else
            x(1) = x(2);
            x(N+2) = x(N+1);
            y = [x(1:ih); Thot];
            dTdx = cat(1,-diff(y),0) /h ;
            dTdx = [dTdx(1:ih); zeros(N+2-ih,1)];
            d2Tdx2 = cat(1,0,diff(diff(x)),0)/(h^2) ;
            dx2 = -mdot/(rho*A)*dTdx+ U*P/(A*rho*cp)*(Tamb-x) + kf/(rho*cp)*d2Tdx2;
        end
    end
end

if t > 6010
    f=0;
end

dx = dx1 + dx2;

end

```

## APPENDIX C IMPLEMENTATION OF HEAT EXCHANGERS

```
function [Thout,Tcout,Qex] = Heat_exchanger(mdothot,mdotcold,Thin,Tcin,cw,cwg)

Aex = 0.322;%0.672;%0.76;
K = 2277;%2182;%; % %500;

if Thin <= Tcin
    mdothot = 0;
end

if mdothot > 0 && mdotcold > 0
    Ch = mdothot*cwg;
    Cc = mdotcold*cw;

    if Ch == Cc
        NTU = Aex*K/Ch;
        epsilon = NTU/(1+NTU);
    else
        Cmin = min(Ch,Cc);
        Cmax = max(Ch,Cc);
        NTU = Aex*K/Cmin;
        Z = Cmin/Cmax;
        epsilon = (1-exp(-NTU*(1-Z)))/(1-Z*exp(-NTU*(1-Z)));
    end
    Qex = Ch*(Thin-Tcin)*epsilon;
    Thout = Thin-Qex/Ch;
    Tcout = Tcin+Qex/Cc;
else
    Thout = Thin;
    Tcout = Tcin;
    Qex = 0;
end

end
```

## APPENDIX D IMPLEMENTATION OF SOLAR PANELS

### ➤ *Matlab code of solar panels*

```
function [Q,Tout,mdot,nu] = SPF(Ti,To,Time,v,w,cwg,on)

nu0 = 0.839;%0.728;%
a1 = 3.47;%3.94;%
a2 = 0.0106;%0.0070;%
A = 20;
mdot = 0;
c = 3700;
% i = 0;
nu = 0;

if Time >= v(1,1) && Time <= v(size(v,1),1)
    Tm = (Ti+To)/2;
    [Ta,G] = findPara(Time,v,w);
    if G > 0
        Tmstar = (Tm - Ta)/G;
        nu = nu0 - a1*Tmstar - a2*G*Tmstar^2;
    end

    if nu <= 0 || on ==0
        Q =0;
        Tout = Ti;
    else
        Q = nu*G*A;
        mdot = 0.05*abs(To-Ti+1)*A/60;
        Tout = Ti + Q/(mdot*c);
        f=0;
    end
end

else
```

```

    Q = 0;
    Tout = Ti;
end
f=0;
end

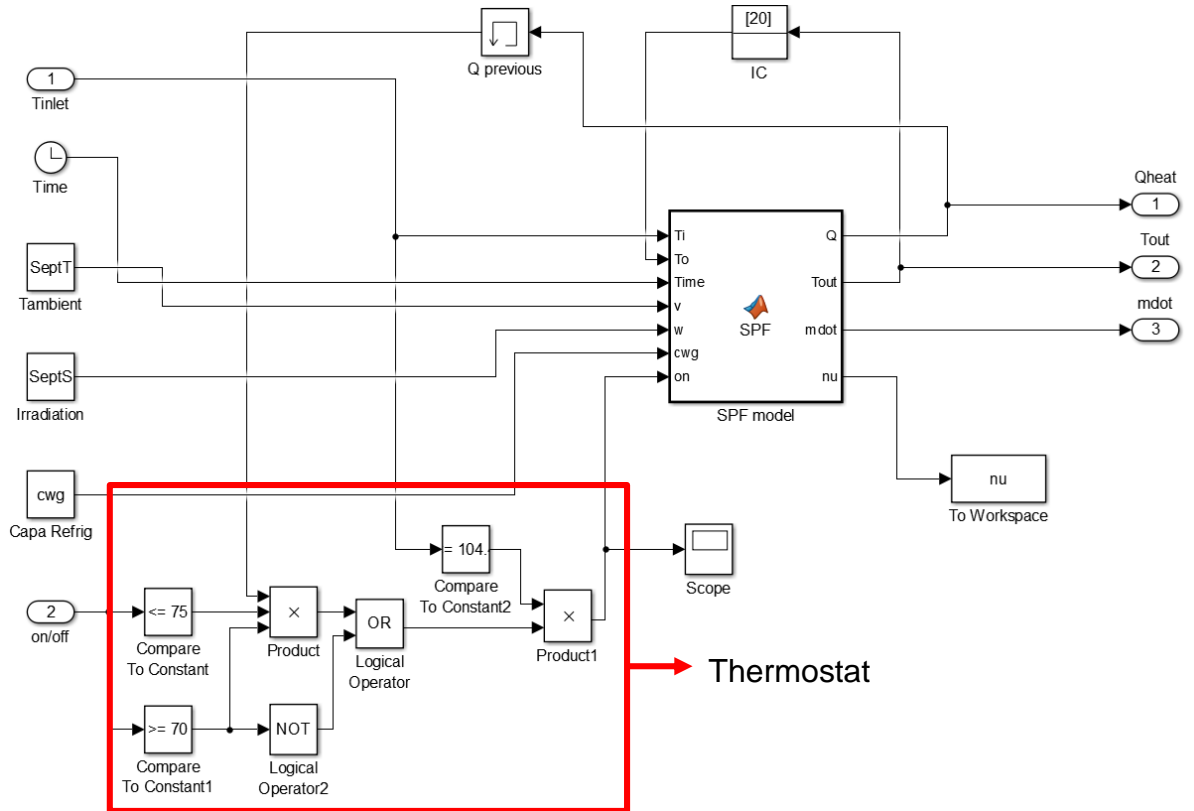
function [Ta,G] = findPara(t,data,w)

i = 1;
while t > data(i,1) && i+1 < size(data,1)
    i = i+1;
end

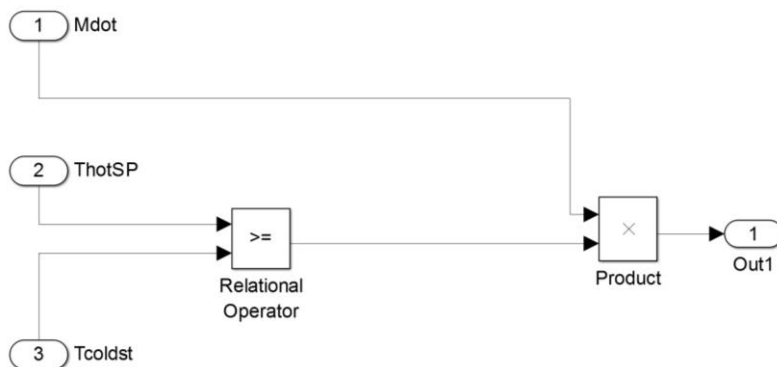
if i < 2
    Ta = data(i,2);
    G = w(i,2);
else
    Ta = (data(i,2)-data(i-1,2))/(data(i,1)-data(i-1,1))*(t-data(i,1))+data(i,2);
    G = (w(i,2)-w(i-1,2))/(w(i,1)-w(i-1,1))*(t-w(i,1))+w(i,2);
end
end

```

➤ **Implementation of the thermostat in the Solar collector block**



➤ **Logic inside the 'Solar heating controller' block**



## APPENDIX E GAS BOILER AND CONTROLLER OF THE GAS HEATING LOOP

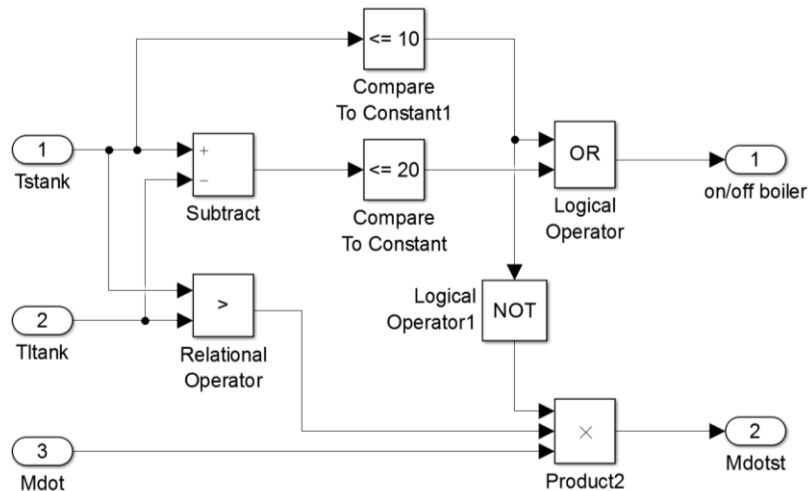
### ➤ Matlab code inside the 'Gas boiler' block

```
function [Tbout,mdotboiler,Q,Qb] = Boiler(Tbin,load,Qprevious,State,QHE)

Tbout = Tbin;
mdotboiler = 0;
Q = 0;
Qb = 0;
nu = 0.8;
QHE = abs(QHE);

if Tbin > 65 || load > 0
elseif (60 <= Tbin) && (Tbin <= 65)
    if Qprevious > 0
        if State == 1;
            mdotboiler = 0.2;
            Qb = nu*61*10^3;
            Tbout = Tbin + Qb/(mdotboiler * 4182);
        elseif QHE > 0
            mdotboiler = 0.2;
        end
    end
elseif Tbin < 60
    mdotboiler = 0.2;
    if State == 1
        mdotboiler = 0.2;
        Qb = nu*61*10^3;
        Tbout = Tbin + Qb/(mdotboiler * 4182);
    elseif QHE > 0
        mdotboiler = 0.2;
    end
end
Q = 2*Qb + QHE;
end
```

### ➤ Logic inside the 'Gas heating controller' block



**APPENDIX F COST OF COMPONENTS OF THE SYSTEM [41]**

Component	Cost (£)
Tank 320l	1188
Tank 400l	1404
Tank 500l	1620
Heat exchanger (733W.K <sup>-1</sup> )	487
Heat exchanger (1466W.K <sup>-1</sup> )	741
Circulation pump for low head	215
Circulation pump for solar collectors	500

**APPENDIX G CAPITAL COST OF SOLAR PRE-HEATING SYSTEMS**

Version	Cost (£)
16m <sup>2</sup> Solex BLUx, tank 320l, heat exchanger (733W.K <sup>-1</sup> )	12162
16m <sup>2</sup> Solex BLUx, tank 320l, heat exchanger (1466W.K <sup>-1</sup> )	12670
16m <sup>2</sup> Riello CSAO 25R, tank 320l, heat exchanger (733W.K <sup>-1</sup> )	15362
16m <sup>2</sup> Riello CSAO 25R, tank 320l, heat exchanger (1466W.K <sup>-1</sup> )	15870
16m <sup>2</sup> Solex BLUx, tank 400l, heat exchanger (733W.K <sup>-1</sup> )	12378
16m <sup>2</sup> Solex BLUx, tank 400l, heat exchanger (1466W.K <sup>-1</sup> )	12886
16m <sup>2</sup> Riello CSAO 25R, tank 400l, heat exchanger (733W.K <sup>-1</sup> )	15578
16m <sup>2</sup> Riello CSAO 25R, tank 400l, heat exchanger (1466W.K <sup>-1</sup> )	16086
20m <sup>2</sup> Solex BLUx, tank 400l, heat exchanger (733W.K <sup>-1</sup> )	14538
20m <sup>2</sup> Solex BLUx, tank 400l, heat exchanger (1466W.K <sup>-1</sup> )	15046
20m <sup>2</sup> Riello CSAO 25R, tank 400l, heat exchanger (733W.K <sup>-1</sup> )	18538
20m <sup>2</sup> Riello CSAO 25R, tank 400l, heat exchanger (1466W.K <sup>-1</sup> )	19046
20m <sup>2</sup> Solex BLUx, tank 400l, heat exchanger (733W.K <sup>-1</sup> )	14754
20m <sup>2</sup> Solex BLUx, tank 400l, heat exchanger (1466W.K <sup>-1</sup> )	15262
20m <sup>2</sup> Riello CSAO 25R, tank 400l, heat exchanger (733W.K <sup>-1</sup> )	18754
20m <sup>2</sup> Riello CSAO 25R, tank 400l, heat exchanger (1466W.K <sup>-1</sup> )	19262